Charmed baryons at Belle and Belle II

Hadron 2025

Jing Yuan (Jilin University, China)
On behalf of Belle and Belle II collaborations
March 28, 2025

Belle and Belle II experiments

- **Belle experiment**
  - e^+e^- collision experiment located @ KEK
  - B factory, built to study B mesons' mixing, decay and CP violation.
  - 1999~2010, 1 ab^{-1} data sample

Belle detector

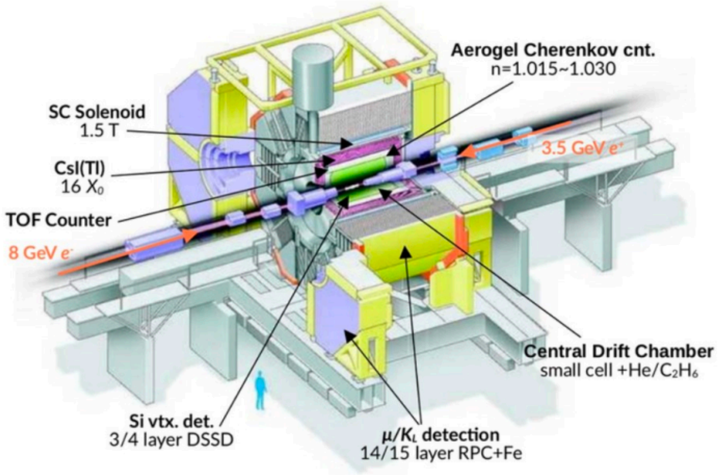

- **Belle II experiment**
  - Updated version of Belle
  - Built to search for new physics out of the standard model
  - Started collecting collision data from 2019

Belle II detector

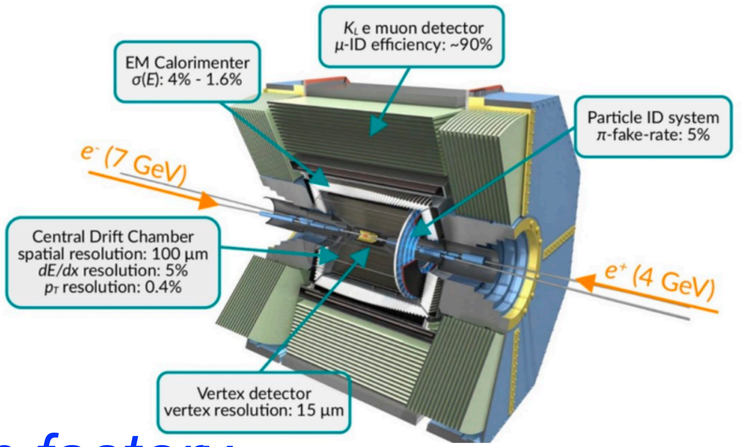

Belle and Belle II are not only B factory, but also τ-charm factory.

How are charm baryons produced @ Belle (II)?

$e^+e^- \to c\bar{c}$

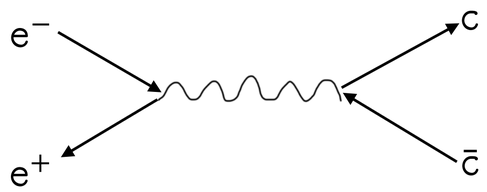

$c\bar{c}$ are produced by e^+e^- directly

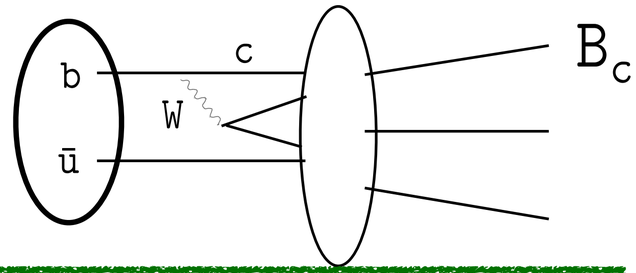

$b \to c$

c is produced by $b \to c$ weak decay

c quark hadronizes into charmed baryon

- ✗ Only relative branching fractions can be measured. The absolute value can be obtained only by reference channel.
- ✗ High level background.
- ✓ Large data sample.

- ✓ The absolute branching fractions can be obtained, because the cross section of $B\bar{B}$ is precisely measured.
- ✓ Clean signal.
- ✗ Small data statistic.
- ✗ Relatively complex analysis procedure.

Selected analyses

- Search for charmed baryons in the $\Lambda_c^+\eta$ system and measurement of the branching fractions of $\Lambda_c(2880)^+$ and $\Lambda_c(2940)^+$ decaying to $\Lambda_c^+\eta$ and pD^0 relative to $\Sigma_c(2455)\pi$
- Search for the semileptonic decays $\Xi_c^0 \to \Xi^0\ell^+\ell^-$
- First observation of $\Lambda\pi^+$ and $\Lambda\pi^-$ signals near the $\bar{K}N\ (I = 1)$ mass threshold in $\Lambda_c^+ \to \Lambda\pi^+\pi^+\pi^-$ decay
- Observations of the singly Cabbibo-suppressed decays $\Xi_c^+ \to pK_S^0$, $\Xi_c^+ \to \Lambda\pi^+$, and $\Xi_c^+ \to \Sigma^0\pi^+$ at Belle and Belle II
- Measurements of the branching fractions of $\Xi_c^0 \to \Xi^0\pi^0$, $\Xi_c^0 \to \Xi^0\eta$, and $\Xi_c^0 \to \Xi^0\eta'$ and asymmetry parameter of $\Xi_c^0 \to \Xi^0\pi^0$
- Search for CP violation and measurement of branching fractions and decay asymmetry parameters for $\Lambda_c^+ \to \Lambda h^+$ and $\Lambda_c^+ \to \Sigma^0 h^+$ $(h = K, \pi)$
- Measurement of the Λ_c^+ lifetime
- Measurement of the Ω_c^+ lifetime

Search for charmed baryons in the $\Lambda_c^+\eta$ and pD^0 system

Belle data, 980 fb^{-1}

*Phys. Rev. D **110**, 032021 (2024)*

- **$\Lambda_c(2880)^+$ and $\Lambda_c(2940)^+$**

  - The $\Lambda_c(2880)^+$ was first observed by CLEO in the $\Lambda_c^+\pi^+\pi^-$ decay mode [1], and later reported by Babar in the pD^0 mass spectrum [2].

  - The $\Lambda_c(2940)^+$ was first seen by BaBar in the pD^0 decay mode [3], and then confirmed by Belle in the $\Sigma_c(2455)\pi$ decay [4].

[1]: M. Artuso et al. (CLEO collaboration), Phys. Rev. Lett. **86**, 4479 (2001).

[2]: B. Aubert et al. (BaBar Collaboration), Phys. Rev. Lett. **98**, 012001 (2007).

- **Why $\Lambda_c^+\eta$ spectrum?**

  - A good channel to search for excited Λ_c^+ baryons.
  - Signal in $\Lambda_c^+\eta$ is likely to be an excited Λ_c^+ rather than Σ_c^+, which is dominated by $\Lambda_c^+\pi$.
  - A narrow enhancement was observed in the pK^- channel near the $\Lambda\eta$ threshold [5].

[3]: B. Aubert et al. (BaBar Collaboration), Phys. Rev. Lett. **98**, 012001 (2007).

[4]: R. Mizuk et al. (Belle Collaboration), Phys. Rev. Lett. **98**, 262001 (2007).

[5]: S. B. Yang et al. (Belle Collaboration), Phys. Rev. D **108**, L031104 (2023).

- **Why pD spectrum?**

  - An analogue to the NK system[6-8].
  - BaBar has reported $\Lambda_c(2880)^+$ and $\Lambda_c(2940)^+$ in the pD^0 mass spectrum [9], while Belle has not investigated it in direct e^+e^- annihilation.

[6]: N. Kaiser, P. B. Siegel, and W. Weise, Nucl. Phys. A **594**, 325 (1995).

[7]: E. Oset and A. Ramos, Nucl. Phys. A **635**, 99 (1998).

[8]: J. A. Oller and U. G. Meißner, Phys. Lett. B **500**, 263 (2001).

[9]: B. Aubert et al. (BaBar Collaboration), Phys. Rev. Lett. **98**, 012001 (2007).

Search for charmed baryons in the $\Lambda_c^+\eta$ and pD^0 system

Belle data, 980 fb^{-1}

Phys. Rev. D ***110***, *032021 (2024)*

- Study for the first time the $\Lambda_c^+\eta$ system and search for singly-charmed baryons, measure relative branching fractions of $\Lambda_c(2880)^+/\Lambda_c(2940)^+ \to \Lambda_c^+\eta/pD^0$.

No obvious $\Lambda_c(2880)^+$ or $\Lambda_c(2940)^+$ signals are seen in $\Lambda_c^+\eta$ spectra.

Clear $\Lambda_c(2880)^+$ and $\Lambda_c(2940)^+$ signals can be seen in pD^0 spectra as well as the $\Sigma_c(2455)\pi$ signal region.

This background is expected and due to the $\Lambda_c(2880)^+ \to \Lambda_c^+\pi^+\pi^-$

$$\frac{\Lambda_c(2880)^+ \to \Lambda_c^+\eta}{\Lambda_c(2880)^+ \to \Sigma_c(2455)\pi} < 0.13 \qquad \frac{\Lambda_c(2940)^+ \to \Lambda_c^+\eta}{\Lambda_c(2940)^+ \to \Sigma_c(2455)\pi} < 1.11$$

$$\frac{\Lambda_c(2880)^+ \to pD}{\Lambda_c(2880)^+ \to \Sigma_c(2455)\pi} = 0.75 \pm 0.03(\text{stat.}) \pm 0.07(\text{syst.})$$

$$\frac{\Lambda_c(2940)^+ \to pD}{\Lambda_c(2940)^+ \to \Sigma_c(2455)\pi} = 3.95 \pm 0.21(\text{stat.}) \pm 0.56(\text{syst.})$$

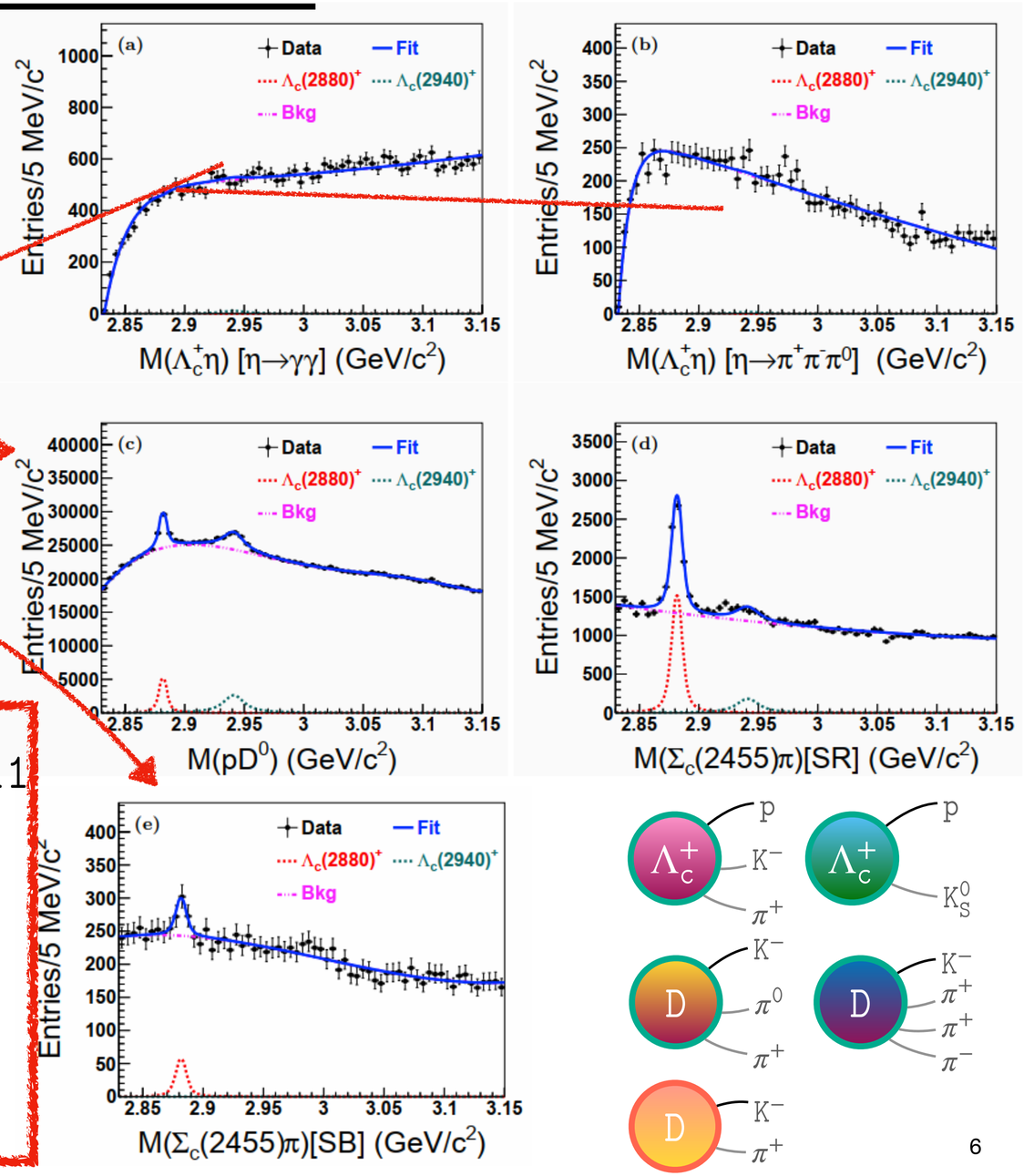

Search for the semileptonic decays $\Xi_c^0 \to \Xi^0 \ell^+ \ell^-$

Belle data, 980 fb^{-1}

*Phys. Rev. D **109**, 052003 (2024)*

- Theoretical study of baryon semileptonic decays is complex due to W-exchange transitions [1-4] and poorly understood hadronic form factors.
- Experimentally, few neutrino-less semileptonic decays of baryons have been observed. Measurements exist for light-baryon octets and bottom baryons ($\Xi^0 \to \Lambda^0 e^+ e^-$, $\Sigma^+ \to p\mu^+\mu^-$ and $\Lambda_b \to \Lambda\mu^+\mu^-$) [5-9], but not for charmed baryons.
- The study of semileptonic decays of baryons provides an opportunity to test the Standard Model, and also can help in the understanding of the recent anomalies in meson FCNC processes.
- If observed, would also allow an LFU test to be performed.

[1]: R. M. Wang, Y. G. Xu, C. Hua, and X. D. Cheng, Phys. Rev. D **103**, 013007 (2021).
[2]: Y.-M. Wang, Y. Li, and C.-D. Lu, Eur. Phys. J. C **59**, 861 (2009).
[3]: T. Mannel and S. Recksiegel, J. Phys. G 24, 979 (1998).
[4]: G. Hiller, M. Knecht, F. Legger, and T. Schietinger, Phys. Lett. B **649**, 152 (2007).
[5]: J. R. Batley et al. (NA48 Collaboration), Phys. Lett. B **650**, 1 (2007).
[6]: H. Park et al.(HyperCP Collaboration), Phys. Rev. Lett. **94**, 021801 (2005).
[7]: T. Aaltonen et al. (CDF Collaboration), Phys. Rev. Lett. **107**, 201802 (2011).
[8]: R. Aaij et al. (LHCb Collaboration), Phys. Lett B **725**, 25 (2013).

No significant signal observed, consistent with SM

experimental:

$$\mathcal{B}(\Xi_c^0 \to \Xi^0 e^+ e^-) < 9.9 \times 10^{-5}$$

$$\mathcal{B}(\Xi_c^0 \to \Xi^0 e^+ e^-) < 6.5 \times 10^{-5}$$

theoretical:

$$\mathcal{B}(\Xi_c^0 \to \Xi^0 e^+ e^-) < 2.35 \times 10^{-6}$$

$$\mathcal{B}(\Xi_c^0 \to \Xi^0 e^+ e^-) < 2.25 \times 10^{-6}$$

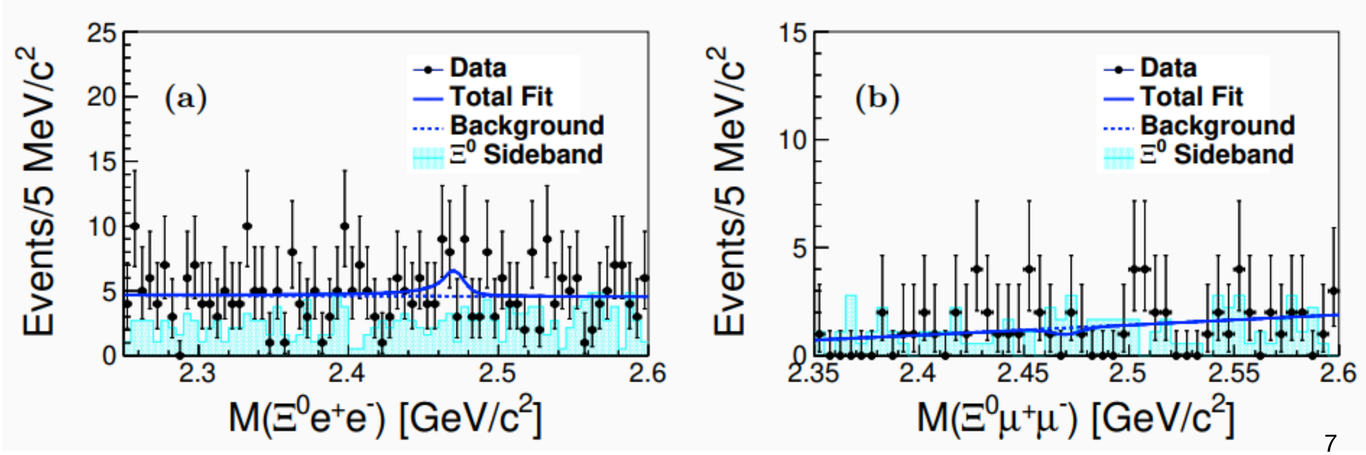

First Observation of $\Lambda\pi^+$ and $\Lambda\pi^-$ Signals near the $\bar{K}N^-$ $(I = 1)$ Mass Threshold in the $\Lambda_c^+ \to \Lambda\pi^+\pi^+\pi^-$ decay

Phys. Rev. Lett ***130****, 151903 (2023)*

Belle data, $980\ fb^{-1}$

- **This is the first time to observe significant signal on $\Lambda\pi^+(\Lambda\pi^-)$ mass spectrum in $\Lambda_c^+ \to \Lambda\pi^+\pi^+\pi^-$ decay channel, which is close to $\bar{K}N$ threshold $(1435\ MeV/c^2)$.**

- Investigate the spectrum structure on $\Lambda\pi^{+(-)}$ mass spectrum above the $\Sigma(1385)$. The traditional quark model did not predict any new excited state of Σ^* near $\Lambda(1405)$, thus the observation of signal can indicate new physics (such as exotic state or threshold effect).

- The interaction of $\bar{K}N$ $(I = 1)$ is related to kaon condensation in neutron stars. It is probably not strong enough to form a bound state, but can produce a virtual state, which can be observed as a threshold cusp [1].

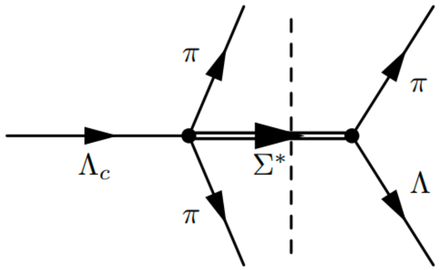

Search for Σ^* state

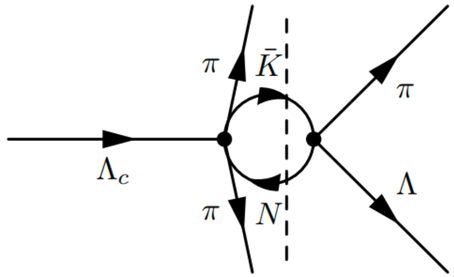

Study $\bar{K}N$ scattering with a cusp

[1]: J. Oller and U.-G. Meißner, Phys. Lett. B **500**, 263 (2001).

First Observation of $\Lambda\pi^+$ and $\Lambda\pi^-$ Signals near the $\bar{K}N^-$ $(I = 1)$ Mass Threshold in the $\Lambda_c^+ \to \Lambda\pi^+\pi^+\pi^-$ decay

*Phys. Rev. Lett **130**, 151903 (2023)*

Belle data, 980 fb^{-1}

Σ^* resonances

TABLE I. Breit-Wigner fitting results. The quoted errors are statistical only.

Mode	$E_{\rm BW}$ [MeV/c^2]	Γ [MeV/c^2]	χ^2 / NDF
$\Lambda\pi^+$	1434.3 ± 0.6	11.5 ± 2.8	74.4/68
$\Lambda\pi^-$	1438.5 ± 0.9	33.0 ± 7.5	92.3/68

$$f_{\rm BW} = \frac{\Gamma/2}{(E - E_{\rm BW})^2 + \Gamma^2/4},$$

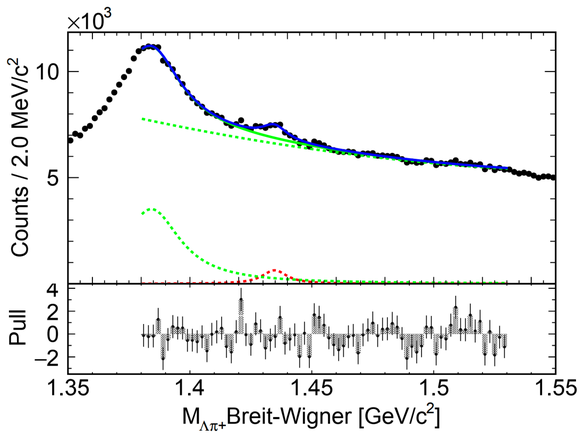

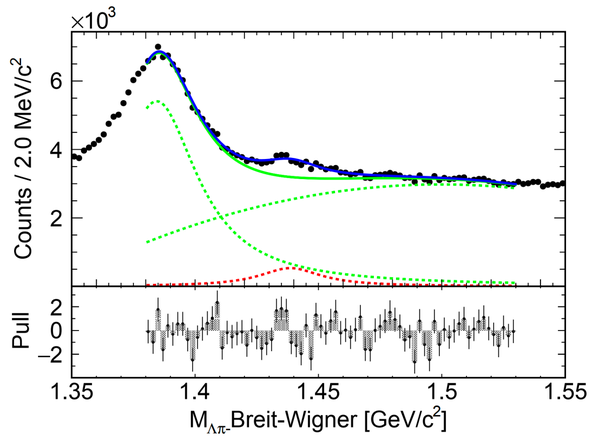

Fit based on the two interpretations.

$\bar{K} - N$ rescattering

TABLE II. Dalitz model fitting results.

Mode	a[fm]	b[fm]	χ^2 / NDF
$\Lambda\pi^+$	0.48 ± 0.32	1.22 ± 0.83	68.9/68
$\Lambda\pi^-$	1.24 ± 0.57	0.18 ± 0.13	78.1/68

By neglecting the Λ_c^+ decay form factor, the $\bar{K}N$ cusp can be related to the $\bar{K} - N$ complex scattering length (A = a+ib) with the Dalitz model

Also tested by Flatte parametrization

a+ib: scattering lengths

$$f_D = \frac{4\pi b}{(1+kb)^2 + (ka)^2}, E > m_{\bar{K}N}$$
$$= \frac{4\pi b}{(1+\kappa a)^2 + (\kappa b)^2}, E < m_{\bar{K}N},$$

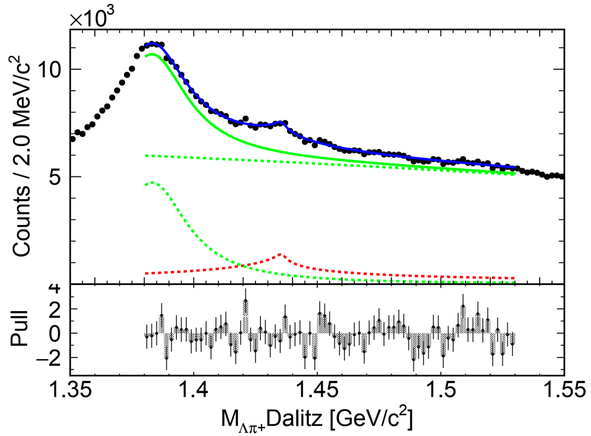

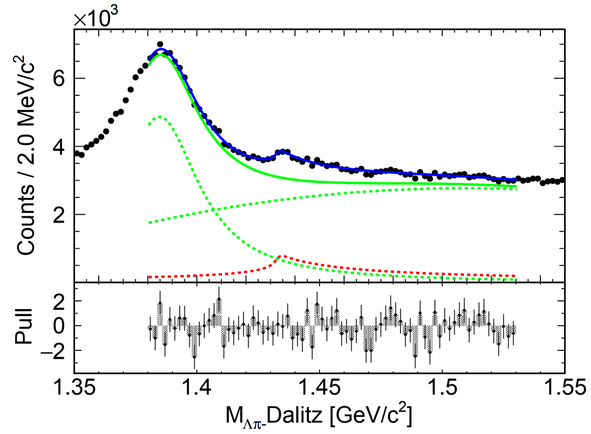

The two fits give similar χ^2 s.

Due to the limitation of the statistic, we can not distinguish between Σ^* resonances and $\bar{K}N$ threshold cusps.

Observations of the singly Cabbibo-suppressed decays $\Xi_c^+ \to pK_S^0$, $\Xi_c^+ \to \Lambda\pi^+$, and $\Xi_c^+ \to \Sigma^0\pi^+$ at Belle and Belle II

Belle data, 980 fb^{-1} + Belle II data 428 fb^{-1}

*JHEP **03** (2025) 061*

- In the last few years, there has been a significant advance in the experimental and theoretical studies of hadronic weak decays of anti-triplet charmed baryons.
- Theoretical calculations for the two-body hadronic weak decays of Ξ_c^+ have been performed based on dynamical model calculations and $SU(3)_F$ flavor symmetry methods. Most of these decay channels have not yet been measured experimentally, especially the singly Cabibbo-suppressed (SCS) decays.
- The $\Xi_c^+ \to \Xi^-\pi^+\pi^+$ is used as the reference channel.

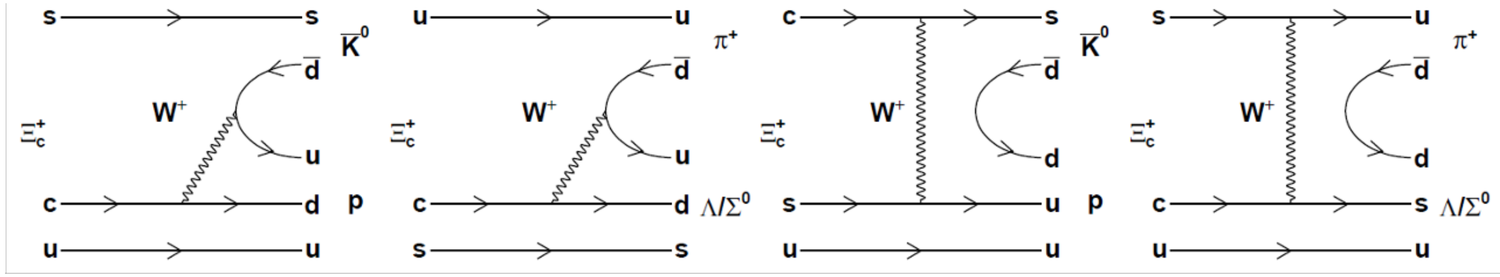

	Belle	Belle II	combined
$\frac{\mathcal{B}(\Xi_c^+\to pK_S^0)}{\mathcal{B}(\Xi_c^+\to\Xi^-\pi^+\pi^+)}$	$(2.36 \pm 0.27 \pm 0.08)\%$	$(2.56 \pm 0.19 \pm 0.11)\%$	$(2.47 \pm 0.16 \pm 0.07)\%$
$\frac{\mathcal{B}(\Xi_c^+\to\Lambda\pi^+)}{\mathcal{B}(\Xi_c^+\to\Xi^-\pi^+\pi^+)}$	$(1.72 \pm 0.29 \pm 0.11)\%$	$(1.47 \pm 0.16 \pm 0.09)\%$	$(1.56 \pm 0.14 \pm 0.09)\%$
$\frac{\mathcal{B}(\Xi_c^+\to\Sigma^0\pi^+)}{\mathcal{B}(\Xi_c^+\to\Xi^-\pi^+\pi^+)}$	$(3.97 \pm 0.42 \pm 0.23)\%$	$(4.26 \pm 0.33 \pm 0.24)\%$	$(4.13 \pm 0.26 \pm 0.22)\%$

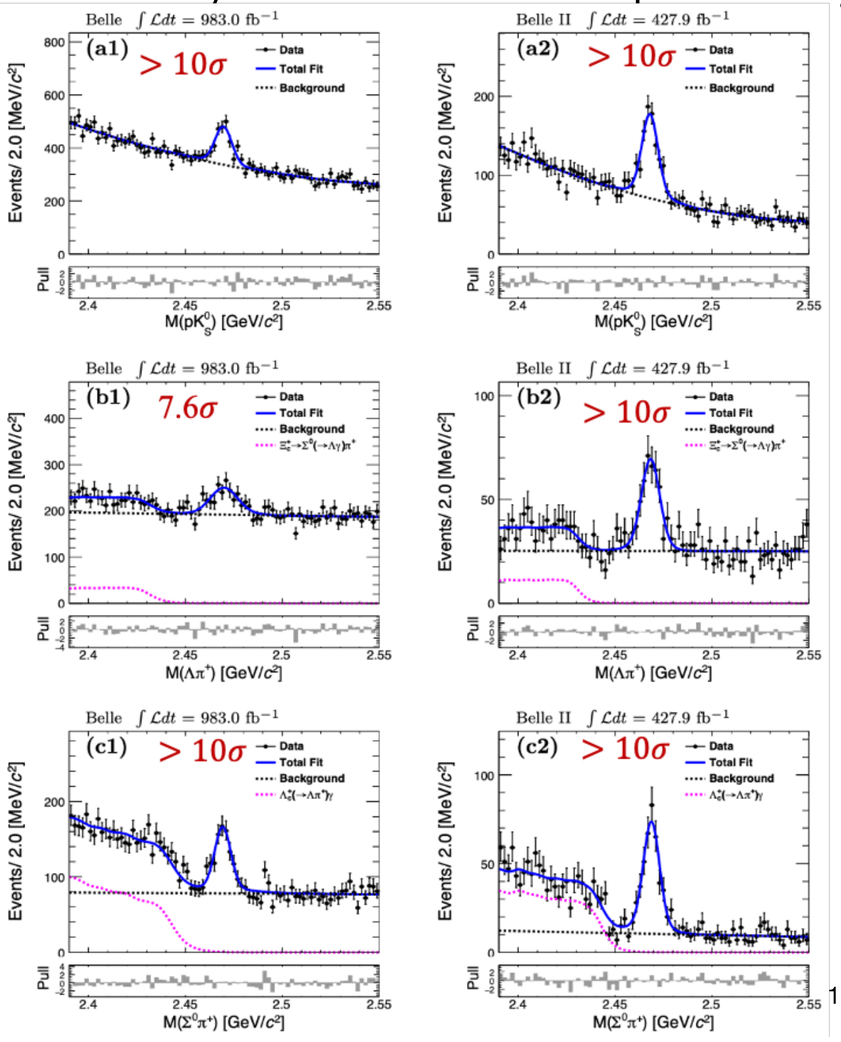

Observations of the singly Cabbibo-suppressed decays $\Xi_c^+ \to pK_S^0$, $\Xi_c^+ \to \Lambda\pi^+$, and $\Xi_c^+ \to \Sigma^0\pi^+$ at Belle and Belle II

Belle data, 980 fb^{-1} + Belle II data 428 fb^{-1}

*JHEP **03** (2025) 061*

Comparisons of measured (a) $\mathcal{B}(\Xi_c^+ \to pK_S^0)$, (b) $\mathcal{B}(\Xi_c^+ \to \Lambda\pi^+)$, and (c) $\mathcal{B}(\Xi_c^+ \to \Sigma^0\pi^+)$ with theoretical predictions [1-11].

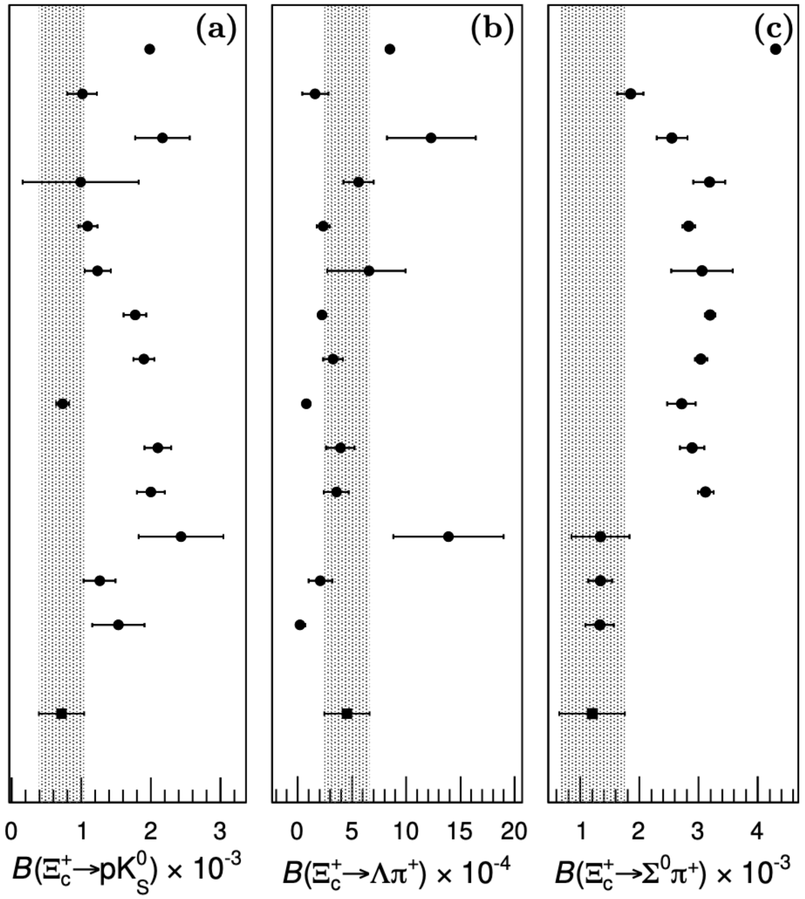

Zou et. al [1]
Geng et. al [2]
Geng et. al [3]
Huang et. al [4]
Zhong et. al (I) [5]
Zhong et. al (II) [5]
Xing et. al (II) [6]
Geng et. al (II) [7]
Liu [8]
Zhong et. al (I) [9]
Zhong et. al (II) [9]
Zhao et. al [10]
Hsiao et. al (I) [11]
Hsiao et. al (II) [11]

Belle and Belle II combined measurement

[1]: J. Zou, F. Xu, G. Meng, and H. Y. Cheng, Two-body hadronic weak decays of antitriplet charmed baryons, Phys. Rev. D **101** (2020) 014011.

[2]: C. Q. Geng, Y. K. Hsiao, C. W. Liu, and T. H. Tsai, Antitriplet charmed baryon decays with SU(3) flavor symmetry, Phys. Rev. D **97** (2018) 073006

[3]: C. Q. Geng, C. W. Liu, and T. H. Tsai, Asymmetries of anti-triplet charmed baryon decays, Phys. Lett. B **794** (2019) 19.

[4]: F. Huang, Z. P. Xing, and X. G. He, A global analysis of charmless two body hadronic decays for anti-triplet charmed baryons, JHEP **03** (2022) 143.

[5]: H. Zhong, F. Xu, Q. Wen, and Y. Gu,Weak decays of antitriplet charmed baryons from the perspective of flavor symmetry, JHEP **02** (2023) 235.

[6]: Z. P. Xing, X. G. He, F. Huang, and C. Yang, Global analysis of measured and unmeasured hadronic two-body weak decays of antitriplet charmed baryons, Phys. Rev. D **108** (2023) 053004.

[7]: C. Q. Geng, X. G. He, X. N. Jin, C. W. Liu, and C. Yang, Complete determination of $SU(3)_F$ amplitudes and strong phase in $\Lambda_c^+ \to \Xi^0 K^+$, Phys. Rev. D **109** (2024) L071302.

[8]: C. W. Liu, Nonleptonic two-body weak decays of charmed baryons, Phys. Rev. D **109** (2024) 033004.

[9]: H. Zhong, F. Xu, and H. Y. Cheng, Analysis of hadronic weak decays of charmed baryons in the topological diagrammatic approach, Phys. Rev. D **109** (2024) 114027.

[10]: H. J. Zhao, Y. L. Wang, Y. K. Hsiao, and Y. Yu, A diagrammatic analysis of two-body charmed baryon decays with flavor symmetry, JHEP **02** (2020) 165.

[11]: Y. K. Hsiao, Y. L. Wang, and H. J. Zhao, Equivalent $SU(3)_f$ approaches for two-body anti-triplet charmed baryon decays, JHEP **09** (2022) 035.

Measurements of the branching fractions of $\Xi_c^0 \to \Xi^0\pi^0$, $\Xi_c^0 \to \Xi^0\eta$, and $\Xi_c^0 \to \Xi^0\eta'$ and asymmetry parameter of $\Xi_c^0 \to \Xi^0\pi^0$

Belle data, 980 fb^{-1} + Belle II data 428 fb^{-1}

JHEP ***10*** *(2024) 045*

Branching fractions

Mode	Belle	Belle II	Combined
$\mathcal{B}(\Xi_c^0 \to \Xi^0\pi^0)/\mathcal{B}(\Xi_c^0 \to \Xi^-\pi^+)$	$0.47 \pm 0.02 \pm 0.03$	$0.51 \pm 0.03 \pm 0.05$	$0.48 \pm 0.02 \pm 0.03$
$\mathcal{B}(\Xi_c^0 \to \Xi^0\eta)/\mathcal{B}(\Xi_c^0 \to \Xi^-\pi^+)$	$0.10 \pm 0.02 \pm 0.01$	$0.14 \pm 0.02 \pm 0.02$	$0.11 \pm 0.01 \pm 0.01$
$\mathcal{B}(\Xi_c^0 \to \Xi^0\eta')/\mathcal{B}(\Xi_c^0 \to \Xi^-\pi^+)$	$0.12 \pm 0.03 \pm 0.01$	$0.06 \pm 0.03 \pm 0.01$	$0.08 \pm 0.02 \pm 0.01$

Asymmetry parameter of $\Xi_c^0 \to \Xi^0\pi^0$

$\cos\theta_{\Xi^0}$	$(-1.0, -0.6)$	$(-0.6, -0.2)$	$(-0.2, 0.2)$	$(0.2, 0.6)$	$(0.6, 1.0)$
Belle	$\frac{260\pm25}{1.40}$	$\frac{296\pm26}{1.29}$	$\frac{266\pm27}{1.14}$	$\frac{265\pm27}{0.99}$	$\frac{224\pm24}{0.71}$
Belle II	$\frac{176\pm18}{2.37}$	$\frac{167\pm18}{2.08}$	$\frac{194\pm20}{1.96}$	$\frac{151\pm17}{1.60}$	$\frac{176\pm17}{1.18}$

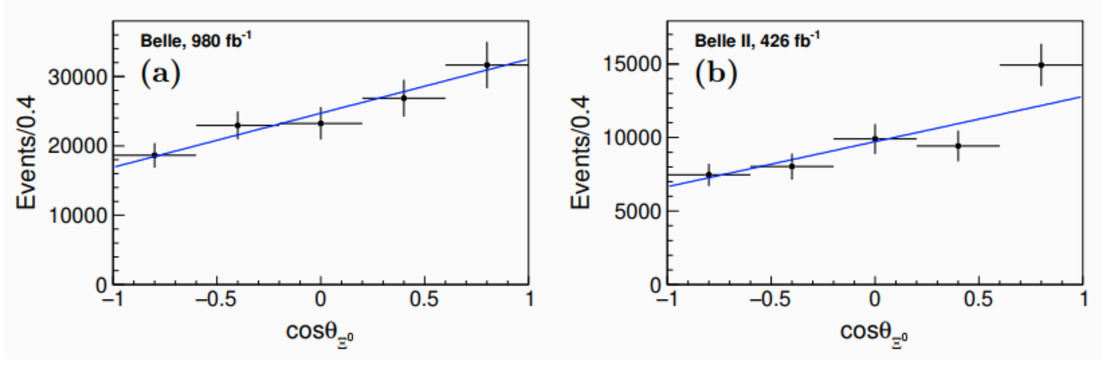

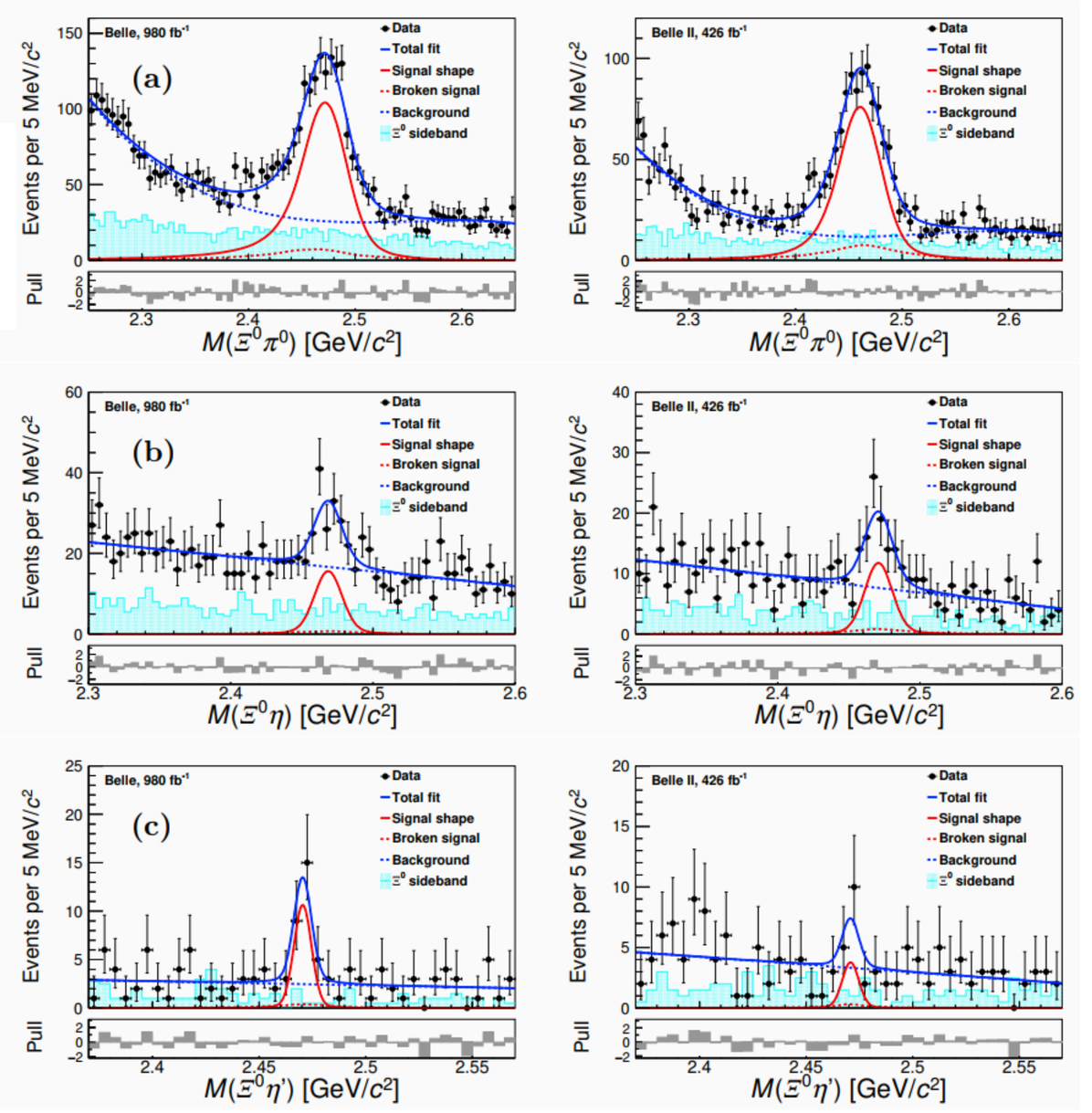

Search for CP violation and measurement of branching fractions and decay asymmetry parameters for $\Lambda_c^+ \to \Lambda h^+$ and $\Lambda_c^+ \to \Sigma^0 h^+$ $(h = K, \pi)$

Belle data, 980 fb^{-1} *Sci. Bull.* ***68****, (2023) 583-592*

- CP violation (CPV) is one of the essential requirements to form the matter-anti-matter asymmetrical universe [1]. In the standard model, the only source of CPV is the single complex phase in the CKM matrix, which is not enough to explain the observed asymmetry.
- The CPV has been observed in open charm mesons and Λ_b^0 decay. An observation of CPV in charm decays much greater than 10^{-3} could indicate new physics beyond the SM [2-5].
- This paper reports A_{CP}^{dir}, A_{CP}^{α} and BF measurements for the SCS decays $\Lambda_c^+ \to \Lambda K^+$ and $\Lambda_c^+ \to \Sigma^0 K^+$, using the CF decays $\Lambda_c^+ \to \Lambda \pi^+$ and $\Lambda_c^+ \to \Sigma^0 \pi^+$ as reference modes.
- The $A_{CP}^{\alpha}(\Lambda \to p\pi^-)$ can be extracted from $A_{CP}^{\alpha}(\mathrm{total}) = (\alpha_{\Lambda_c^+}\alpha_- - \alpha_{\bar{\Lambda}_c^-}\alpha^+)/(\alpha_{\Lambda_c^+}\alpha_- + \alpha_{\bar{\Lambda}_c^-}\alpha^+)$ from CF reference channels, with $\alpha_{\Lambda_c^+} = -\alpha_{\bar{\Lambda}_c^-}$ (SM).

[1]: A.D. Sakharov, Violation of CP Invariance, C asymmetry, and baryon asymmetry of the universe, Pisma Zh. Eksp. Teor. Fiz. **5** (1967) 32.

[2]: D. Delepine, G. Faisel and C.A. Ramirez, Direct CP violation in D+ ! K0(K¯ 0)π+ decays as a probe for new physics, Eur. Phys. J. C **80** (2020) 596

[3]: A. Dery and Y. Nir, Implications of the LHCb discovery of CP violation in charm decays, JHEP **12** (2019) 104

[4]: M. Chala, A. Lenz, A.V. Rusov and J. Scholtz, ΔA_{CP} within the Standard Model and beyond, JHEP **07** (2019) 161.

[5]: M. Saur and F.-S. Yu, Charm CP V : observation and prospects, Sci. Bull. **65** (2020) 1428.

Search for CP violation and measurement of branching fractions and decay asymmetry parameters for $\Lambda_c^+ \to \Lambda h^+$ and $\Lambda_c^+ \to \Sigma^0 h^+$ ($h = K, \pi$)

Belle data, 980 fb^{-1} *Sci. Bull.* ***68****, (2023) 583-592*

Using $1 \mp A_\epsilon^{h^+}$ as weight factor to cover the $K^+(\pi^+)$ detection efficiency asymmetry.

$$A_{\rm raw} = \frac{N(\Lambda_c^+ \to f) - N(\bar{\Lambda}_c^- \to \bar{f})}{N(\Lambda_c^+ \to f) + N(\bar{\Lambda}_c^- \to \bar{f})}$$

$$A_{\rm raw} = A_{CP}^{\Lambda_c^+ \to \Lambda K^+} + A_{CP}^{\Lambda \to p\pi^-} + A_\varepsilon^\Lambda + A_\varepsilon^{K^+} + A_{\rm FB}^{\Lambda_c^+}$$

Forward-background asymmetry of Λ_c^+ production

$$A_{\rm raw}^{\rm corr}(\Lambda_c^+ \to \Lambda K^+) - A_{\rm raw}^{\rm corr}(\Lambda_c^+ \to \Lambda\pi^+) = A_{CP}^{\rm dir}(\Lambda_c^+ \to \Lambda K^+) - A_{CP}^{\rm dir}(\Lambda_c^+ \to \Lambda\pi^+)\,.$$

Cabibbo-flavoured process, no dir-CP violation in SM.

No evidence of charm CP violation is found.

$$A_{CP}^{\rm dir}(\Lambda_c^+ \to \Lambda K^+)$$

$$A_{CP}^{\rm dir}(\Lambda_c^+ \to \Lambda K^+) = (+2.1 \pm 2.6 \pm 0.1)\%$$
$$A_{CP}^{\rm dir}(\Lambda_c^+ \to \Sigma^0 K^+) = (+2.5 \pm 5.4 \pm 0.4)\%$$

This is the first direct CP asymmetry measurement for SCS two-body decays of charmed baryons.

$$\frac{\mathcal{B}(\Lambda_c^+ \to \Lambda K^+)}{\mathcal{B}(\Lambda_c^+ \to \Lambda\pi^+)} = (5.05 \pm 0.13 \pm 0.09)\% \qquad \frac{\mathcal{B}(\Lambda_c^+ \to \Sigma^0 K^+)}{\mathcal{B}(\Lambda_c^+ \to \Sigma^0\pi^+)} = (2.78 \pm 0.15 \pm 0.05)\%$$

$$\mathscr{B}(\Lambda_c^+ \to \Lambda K^+) = (6.57 \pm 0.17 \pm 0.11 \pm 0.35) \times 10^{-4}$$
$$\mathscr{B}(\Lambda_c^+ \to \Sigma^0 K^+) = (3.58 \pm 0.19 \pm 0.06 \pm 0.19) \times 10^{-4}$$

$$\frac{\mathcal{B}_{\rm sig}}{\mathcal{B}_{\rm ref}} = \frac{N_{\rm sig}/\varepsilon_{\rm sig}}{N_{\rm ref}/\varepsilon_{\rm ref}}$$

Branching fractions

Search for CP violation and measurement of branching fractions and decay asymmetry parameters for $\Lambda_c^+ \to \Lambda h^+$ and $\Lambda_c^+ \to \Sigma^0 h^+$ ($h = K, \pi$)

Belle data, 980 fb^{-1} *Sci. Bull.* **68**, (2023) 583-592

α parameter extraction

corrected bin-by-bin with the signal efficiencies

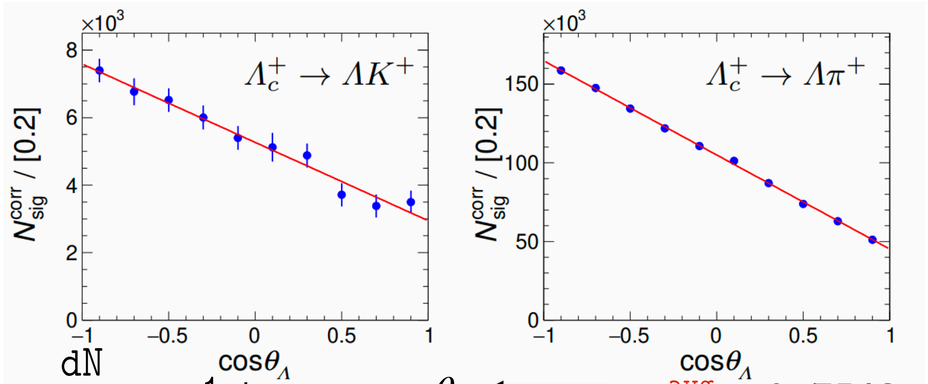

$$\frac{dN}{d\cos\theta_A} \propto 1 + \alpha_{\Lambda_c^+}\alpha_\Lambda \cos\theta_A \longleftarrow \alpha_\Lambda^{avg} = 0.7542 \pm 0.0026$$

$$\begin{aligned}
\alpha^{avg}_{\Lambda_c^+}(\Lambda_c^+ \to \Lambda K^+) &= -0.585 \pm 0.049 \pm 0.018\,, \\
\alpha^{avg}_{\Lambda_c^+}(\Lambda_c^+ \to \Lambda \pi^+) &= -0.755 \pm 0.005 \pm 0.003\,, \\
\alpha^{avg}_{\Lambda_c^+}(\Lambda_c^+ \to \Sigma^0 K^+) &= -0.54 \pm 0.18 \pm 0.09\,, \\
\alpha^{avg}_{\Lambda_c^+}(\Lambda_c^+ \to \Sigma^0 \pi^+) &= -0.463 \pm 0.016 \pm 0.008\,,
\end{aligned}$$

Consistent with the current world average, with better precision.

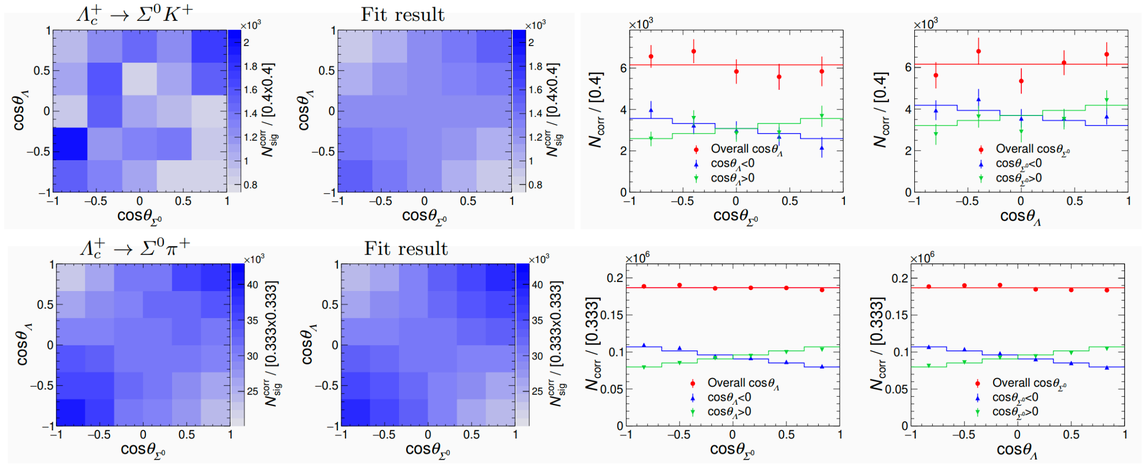

$$\frac{dN}{d\cos\theta_\Sigma^0 d\cos\theta_A} \propto 1 + \alpha_{\Lambda_c^+}\alpha_\Lambda \cos\theta_\Sigma^0 \cos\theta_A$$

The first measurement of hyperon CPV searches in CF charm decays. No evidence of Λ-hyperon CPV is found.

Measure the A_{CP}^{α} in $\Lambda_c^+ \to \Lambda h^+$ and $\Lambda_c^+ \to \Sigma^0 h^+$

Channel	$\alpha_{\Lambda_c^+}\alpha_-$	$\alpha_{\Lambda_c^-}\alpha_+$	$\alpha_{\Lambda_c^+}$	$\alpha_{\bar{\Lambda}_c^-}$	A_{CP}^{α}	W.A. A_{CP}^{α}
$\Lambda_c^+ \to \Lambda K^+$	-0.425 ± 0.053	-0.448 ± 0.053	$-0.566 \pm 0.071 \pm 0.028$	$0.592 \pm 0.070 \pm 0.079$	$-0.023 \pm 0.086 \pm 0.071$	–
$\Lambda_c^+ \to \Lambda \pi^+$	-0.590 ± 0.006	-0.570 ± 0.006	$-0.784 \pm 0.008 \pm 0.006$	$0.754 \pm 0.008 \pm 0.018$	$+0.020 \pm 0.007 \pm 0.014$	-0.07 ± 0.22
$\Lambda_c^+ \to \Sigma^0 K^+$	-0.43 ± 0.18	-0.37 ± 0.21	$-0.58 \pm 0.24 \pm 0.09$	$0.49 \pm 0.28 \pm 0.14$	$+0.08 \pm 0.35 \pm 0.14$	–
$\Lambda_c^+ \to \Sigma^0 \pi^+$	-0.340 ± 0.016	-0.358 ± 0.017	$-0.452 \pm 0.022 \pm 0.023$	$0.473 \pm 0.023 \pm 0.035$	$-0.023 \pm 0.034 \pm 0.030$	–

Search for hyperon CPV in $\Lambda \to p\pi$ in CF modes

$$A_{CP}^{\alpha}(\Lambda \to p\pi^-) = +0.013 \pm 0.007 \pm 0.011$$

Measurement of the Λ_c^+ lifetime

Belle II on/off-resonance data, $207.2\ \mathrm{fb}^{-1}$

*PRL **130**, (2023) 071802*

- Precise measurements of weakly decaying charm or bottom hadrons can help to search for physics beyond the standard model.
- The the heavy quark expansion (HQE) is an effective model to describe strong interactions at low energy, which provides a consistent framework for bottom hadrons. But for charm hadron lifetimes, HQE is not able to describe them satisfactorily [1~3].
- A precise, absolute measurement by Belle II may help to resolve the tension between Λ_c^+ lifetime measurements at e^+e^- colliders and other experiments and will substantially improve the world average [4~12].
- We report a precise measurement of the Λ_c^+ lifetime using $\Lambda_c^+ \to pK^-\pi^+$ decays reconstructed in data collected at or near the $\Upsilon(4S)$ resonance.

[1]: R. Aaij et al. (LHCb Collaboration), Phys. Rev. Lett. **121**, 092003 (2018), arXiv:1807.02024 [hep-ex] .
[2]: R. Aaij et al. (LHCb Collaboration), Phys. Rev. D **100**, 032001 (2019), arXiv:1906.08350 [hep-ex] .
[3]: R. Aaij et al. (LHCb Collaboration), Science Bulletin **67**, 479 (2022)
[4]:R. Aaij et al. (LHCb Collaboration), Phys. Rev. D **100**, 032001 (2019), arXiv:1906.08350 [hep-ex] .
[5]: R. Aaij et al. (LHCb Collaboration), Science Bulletin **67**, 479 (2022).
[6]: P. A. Zyla et al. (Particle Data Group), PTEP 2020, 083C01 (2020).
[7] J. M. Link et al. (FOCUS Collaboration), Phys. Rev. Lett. **88**, 161801 (2002), arXiv:hep-ex/0202001 .
[8] A. Kushnirenko et al. (SELEX Collaboration), Phys. Rev. Lett. **86**, 5243 (2001), arXiv:hep-ex/0010014.
[9] A. H. Mahmood et al. (CLEO Collaboration), Phys. Rev. Lett. **86**, 2232 (2001), arXiv:hep-ex/0011049.
[10] F. Abudin´en et al. (Belle II Collaboration), Phys. Rev. Lett. **127**, 211801 (2021), arXiv:2108.03216 [hep-ex] .
[11] T. Abe et al. (Belle II Collaboration), (2010), arXiv:1011.0352 [physics.ins-det] .
[12] K. Akai, K. Furukawa, and H. Koiso, Nucl. Instrum. Meth. A 907, 188 (2018), arXiv:1809.01958 [physics.acc-ph] .

Measurement of the Λ_c^+ lifetime

Belle II on/off-resonance data, $207.2\ \mathrm{fb}^{-1}$

*PRL **130**, (2023) 071802*

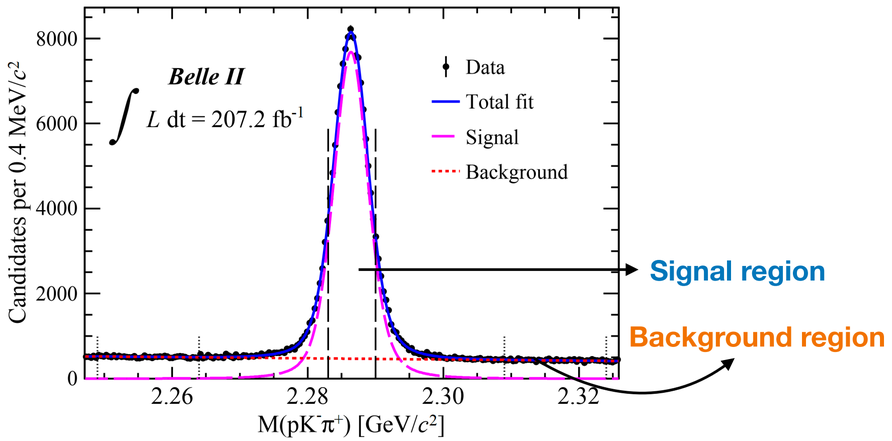

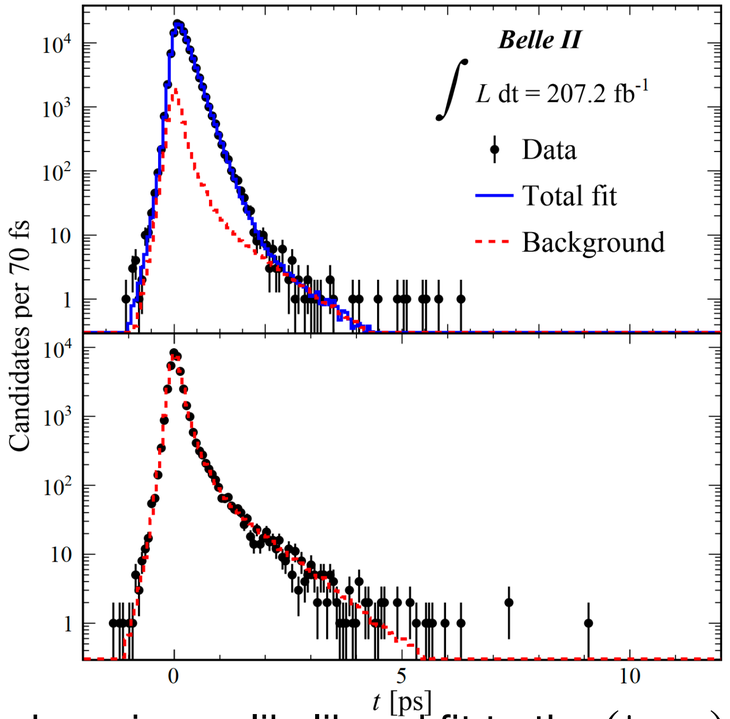

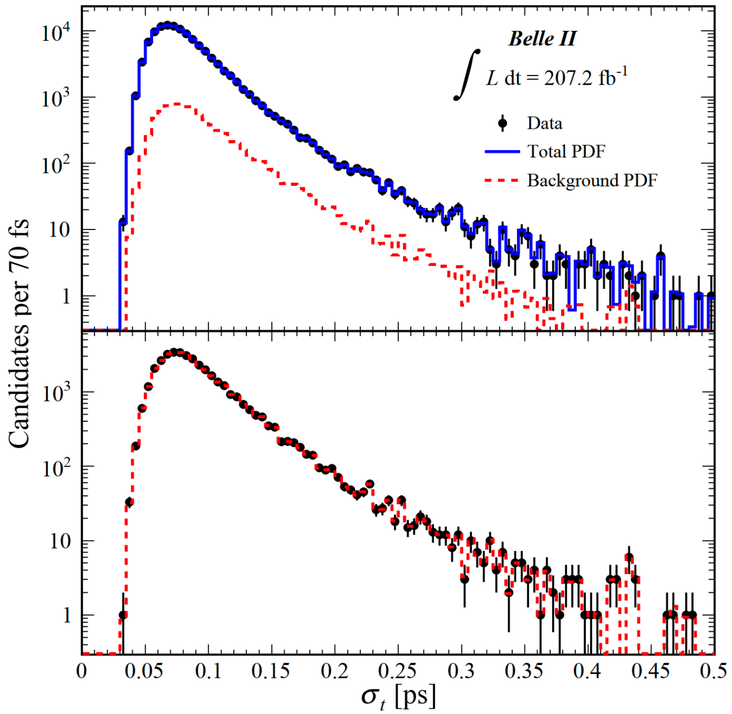

- The Λ_c^+ lifetime is measured with an 2D unbinned maximum-likelihood fit to the (t, σ_t) distribution for events in the signal region.
  - Signal PDF: 1) Exponential function in t convolved with a Gaussian resolution function, which depends on σ_t; 2) PDF for σ_t is a histogram template from background-subtracted signal candidates.
  - Background PDF: Empirical model of the sideband data
- To better constrain the background, a simultaneous fit to the events in the signal region and sidebands is performed.

$$\tau(\Lambda_c^+) = 203.20 \pm 0.89(\mathrm{stat}) \pm 0.77(\mathrm{sys})\ \mathrm{fs}$$

Most precise

Measurement of the Ω_c^0 lifetime

Belle II on/off-resonance data, $207.2\ \mathrm{fb}^{-1}$

*PRD **107**, (2023) L031103*

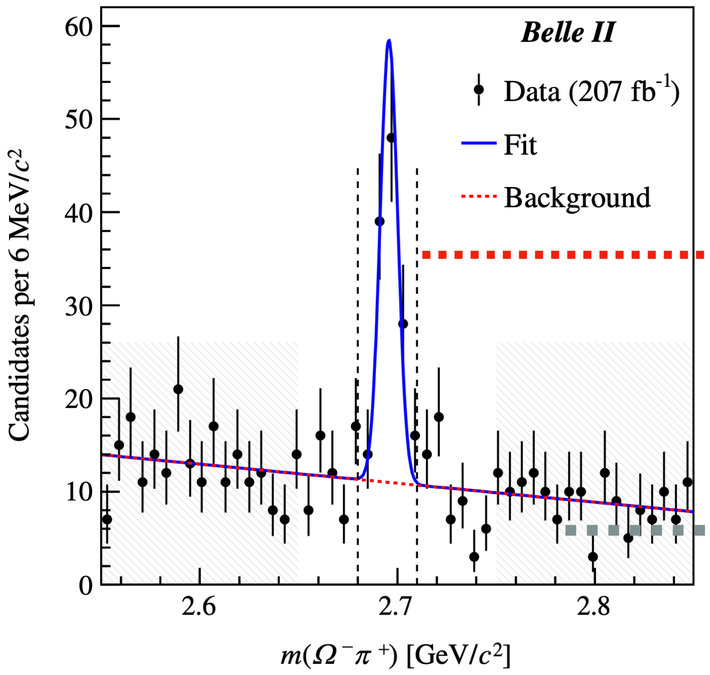

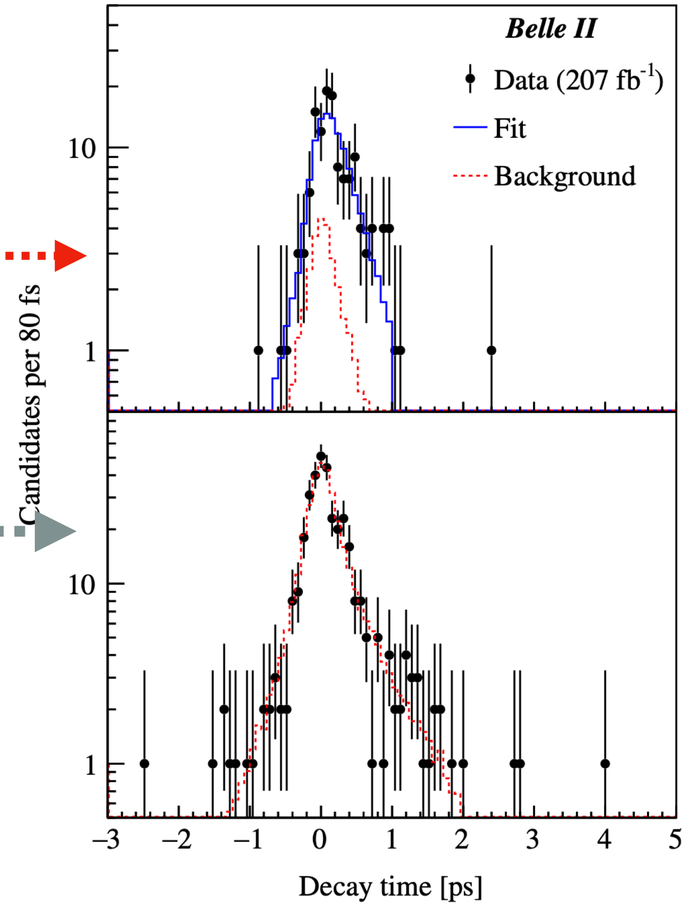

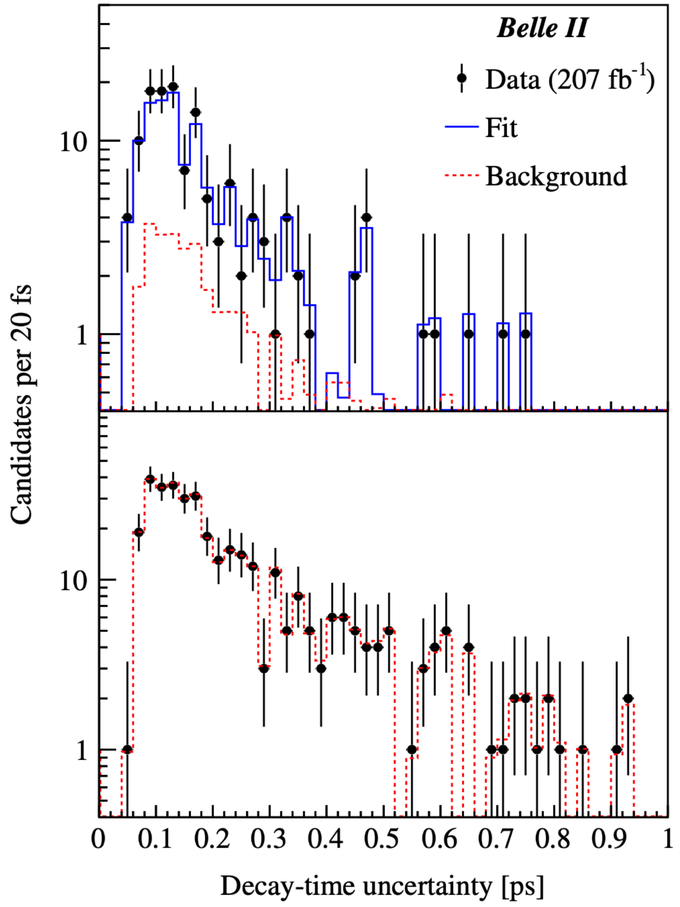

$$\tau(\Omega_c^+) = 243 \pm 48(\mathrm{stat}) \pm 11(\mathrm{sys})\ \mathrm{fs}$$

- This new result is consistent with the LHCb average of 273.5 ± 12.4 fs, and inconsistent with the pre-LHCb world average of 69 ± 12 fs.
- **Confirms that the Ω_c^0 is not the shortest-lived weakly decaying charmed baryon.**

Summary

- Belle's enduring legacy
  - Continues to yield critical insights in charm hadron dynamics even 10+ years post-data-taking
  - Maintains relevance through innovative analysis of its 980 fb^{-1} dataset
- Belle II’s improvement
  - With enhanced of vertex resolution, Belle II has a improved detection precision.
  - Enabling unprecedented precision in charm flavor physics, CP violation studies, and beyond the Standard Model searches.
  - Started run2 taking.

Thank you!

Back Up

Search for charmed baryons in the $\Lambda_c^+\eta$ and pD^0 system

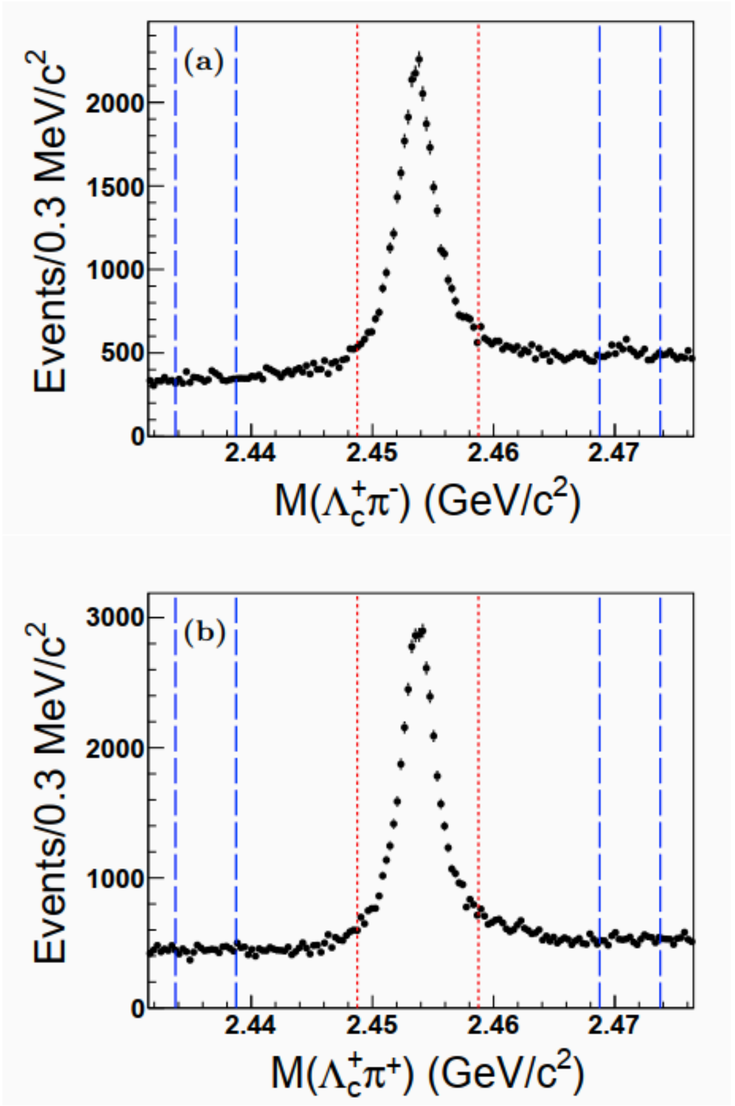

FIG. 1: Invariant-mass distributions of (a) $\Lambda_c^+\pi^-$ and (b) $\Lambda_c^+\pi^+$. Regions between the two red dotted lines are the $\Sigma_c(2455)$ signal regions, and regions between the two blue long-dashed lines are the $\Sigma_c(2455)$ sideband regions.

Search for charmed baryons in the $\Lambda_c^+\eta$ and pD^0 system

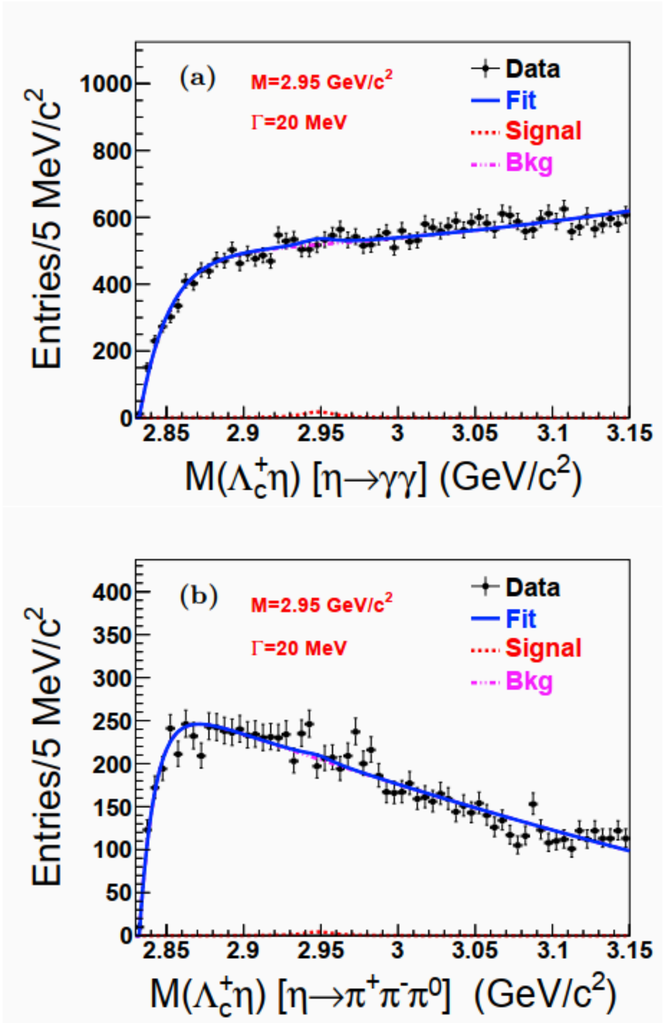

FIG. 2: An example of the simultaneous fit to the $M(\Lambda_c^+\eta)$ spectra with (a) $\eta \to \gamma\gamma$ and (b) $\eta \to \pi^0\pi^+\pi^-$ (points with statistical uncertainties). The blue solid curves represent the result of the fit. The red dashed curves represent a hypothetical excited Λ_c state with $M = 2.95$ GeV/c^2 and $\Gamma = 20$ MeV, while the magenta dash-dotted curves represent the background.

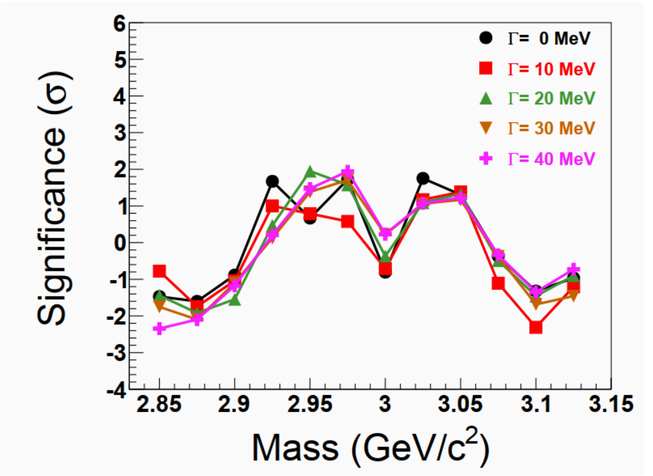

FIG. 3: Statistical significances for the various excited Λ_c^+ hypotheses considered.

We constrain the signal mass and width to be identical for the two η decay modes, and fix the signal mass to be a value from 2.850 to 3.125 GeV/c^2 in steps of 25 MeV/c^2. The signal width is fixed to 0, 10, 20, 30, and 40 MeV for each fixed mass. The ratio of signal yields for the $\eta \to \gamma\gamma$ mode relative to those for the $\eta \to \pi^0\pi^+\pi^-$ mode is calculated by the product of detection efficiencies and the known η branching fractions [26], and is fixed in the fit. This ratio decreases from 5.4 to 2.7 as the signal mass increases from 2.850 to 3.125 GeV/c^2. Figure 2 shows an example of the fit with the signal mass and width fixed to 2.95 GeV/c^2 and 20 MeV, respectively.

Search for the semileptonic decays $\Xi_c^0 \to \Xi^0 \ell^+ \ell^-$

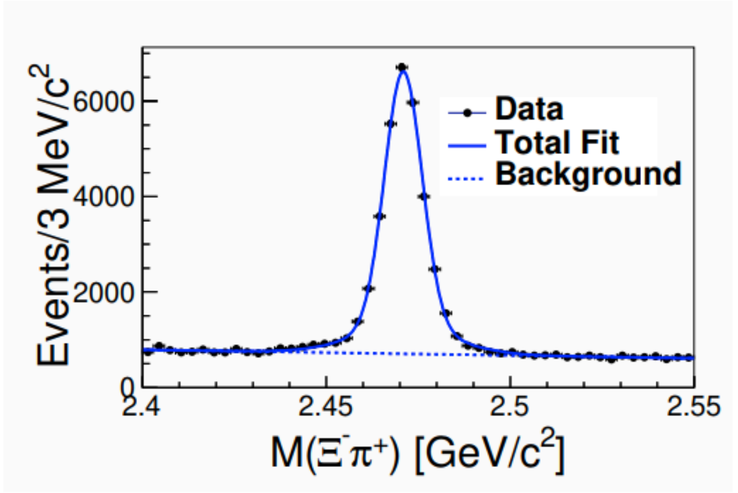

FIG. 1: The invariant-mass distribution of $\Xi^-\pi^+$ combinations in data. The dots with error bar represent the data, the solid curve shows the best-fit result, and the blue dashed curve shows the fitted backgrounds.

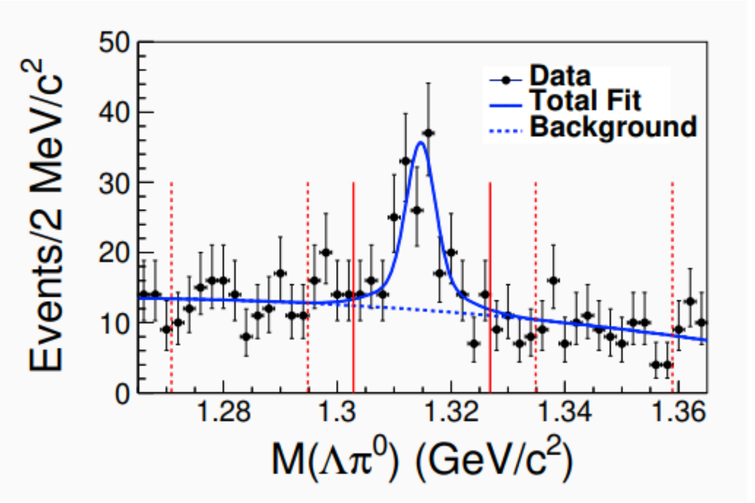

FIG. 2: The invariant-mass distributions of $\Xi^0 \to \Lambda\pi^0$ candidates before combining with the $\ell^+\ell^-$ pairs in the selected Ξ_c^0 signal regions in the data. The dots with error bars represent the data, the solid curve shows the total best-fit result, the dashed curve shows the background shape, and the solid and dashed lines show the signal and sideband regions of Ξ^0 candidates, respectively.

Here, a double Gaussian function models the signal shape, and a second-order polynomial provides the background.

The signal shape parameters are fixed to the values found in signal MC, while the background parameters are free in the fit.

Search for the semileptonic decays $\Xi_c^0 \to \Xi^0 \ell^+ \ell^-$

- To take energy loss due to bremsstrahlung into account, the shapes of correctly reconstructed Ξ_c^0 candidates are described by two Crystal Ball functions for the dielectron mode. In contrast, a double-Gaussian function is used as the signal shape for the di-muon mode.
- Broken signal is mainly due to incorrectly selected photons in Ξ^0 reconstruction. we extract the shape of the broken signal from MC simulation via Rookeyspdf, and treat it as a distinct component in the final Ξ_c^0 signal yield extraction.

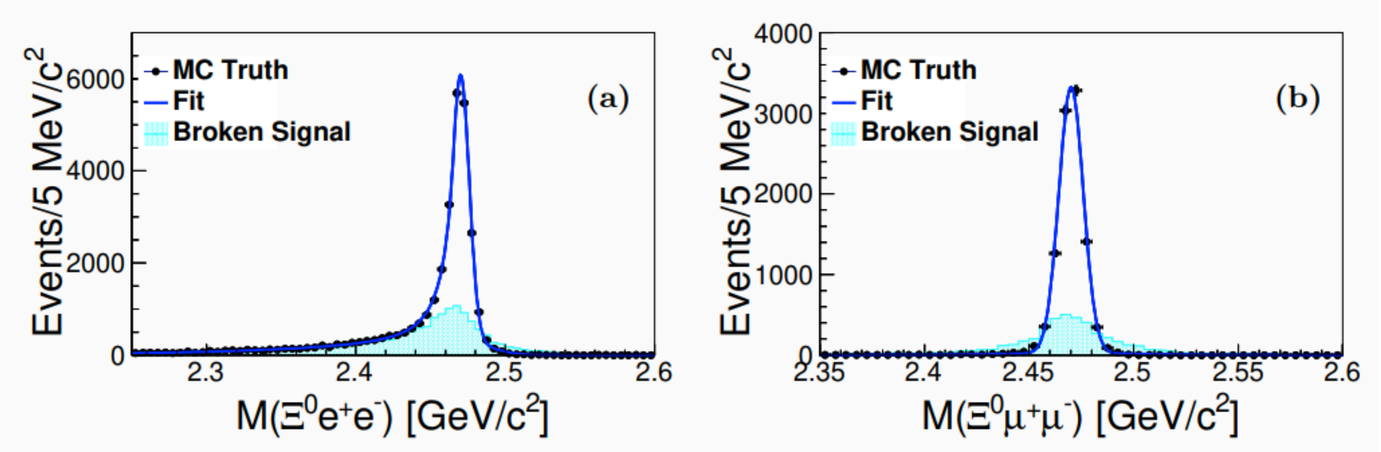

FIG. 3: The invariant-mass distributions of (a) $\Xi^0 e^+ e^-$ and (b) $\Xi^0 \mu^+ \mu^-$ combinations in signal MC simulation. Points with error bars show the correctly reconstructed signal, the blue solid curves show the results of the fit to the signal shape, and the cyan shaded histograms show the broken signal distributions.

Search for the semileptonic decays $\Xi_c^0 \to \Xi^0 \ell^+ \ell^-$

- For the fits to data, the signal shapes are taken from the fits to the signal MC samples above with all the parameters fixed. The width of the signal shape is multiplied by a correction factor.
- The broken signal shape is taken from the MC simulation as described above, and the ratio of the broken signal to correctly reconstructed signal events is fixed.

TABLE I: The summarized values for branching fraction measurements of $\Xi_c^0 \to \Xi^0 \ell^+ \ell^-$ decays. Here, $N^{\rm fit}$ is the fitted signal yield, $N^{\rm UL}$ is the 90% credibility upper limit on the number of signal events from data before considering systematic uncertainties, $\mathcal{B}^{\rm UL}/\mathcal{B}(\Xi_c^0 \to \Xi^-\pi^+)$ and $\mathcal{B}^{\rm UL}$ are the 90% credible upper limits on the relative and absolute branching fractions, respectively, for the $\Xi_c^0 \to \Xi^0 \ell^+ \ell^-$ decays with systematic uncertainties included, and $\mathcal{B}(\Xi_c^0 \to \Xi^-\pi^+) = (1.43 \pm 0.32)\%$ is taken from the Particle Data Group [29].

Modes	$\Xi_c^0 \to \Xi^0 e^+ e^-$	$\Xi_c^0 \to \Xi^0 \mu^+ \mu^-$
Efficiency (%)	1.58	0.53
$N^{\rm fit}$	9.1±7.1	−0.9±2.1
$N^{\rm UL}$	19.9	4.5
$\mathcal{B}^{\rm UL}/\mathcal{B}(\Xi_c^0 \to \Xi^-\pi^+)$	6.7×10^{-3}	4.3×10^{-3}
$\mathcal{B}^{\rm UL}$	9.9×10^{-5}	6.5×10^{-5}

$$\mathcal{B}^{\rm UL}(\Xi_c^0 \to \Xi^0 \ell^+ \ell^-)/\mathcal{B}(\Xi_c^0 \to \Xi^-\pi^+) = \frac{N^{\rm UL}(\Xi_c^0 \to \Xi^0 \ell^+ \ell^-)}{N^{\rm obs}(\Xi_c^0 \to \Xi^-\pi^+)} \times \frac{\varepsilon(\Xi_c^0 \to \Xi^-\pi^+)}{\varepsilon(\Xi_c^0 \to \Xi^0 \ell^+ \ell^-)} \times \frac{\mathcal{B}(\Xi^- \to \Lambda\pi^-)}{\mathcal{B}(\Xi^0 \to \Lambda\pi^0)}$$

TABLE II: The multiplicative systematic uncertainties (%) on the measurements of relative and absolute branching fractions.

Source	$\Xi_c^0 \to \Xi^0 e^+ e^-$	$\Xi_c^0 \to \Xi^0 \mu^+ \mu^-$
Particle ID	3.5	5.5
π^0 selection	3.3	3.0
$\mathcal{B}(\Xi_c^0 \to \Xi^-\pi^+)$	22.4	22.4
Fit of reference mode	0.7	0.7
Total $[\mathcal{B}(\Xi_c^0 \to \Xi^0 \ell^+ \ell^-)/\mathcal{B}(\Xi_c^0 \to \Xi^-\pi^+)]$	4.9	6.3
Total $[\mathcal{B}(\Xi_c^0 \to \Xi^0 \ell^+ \ell^-)]$	23.0	23.3

TABLE III: The detection efficiencies (%) in $(M^2_{e^+e^-}, M^2_{\Xi^0 e^+})$ bins for the $\Xi_c^0 \to \Xi^0 e^+ e^-$ decay mode.

	$M^2_{\Xi^0 e^+}$ (GeV$^2/c^4$)						
$M^2_{e^+e^-}$ (GeV^2/c^4)	[1.4, 2.1]	[2.1, 2.8]	[2.8, 3.5]	[3.5, 4.2]	[4.2, 4.9]	[4.9, 5.6]	[5.6, 6.3]
[0,0.15]	0.39 ± 0.01	0.98 ± 0.01	1.53 ± 0.01	1.69 ± 0.01	1.57 ± 0.01	1.03 ± 0.01	0.39 ± 0.01
[0.15,0.3]	0.65 ± 0.01	1.20 ± 0.01	1.65 ± 0.01	1.78 ± 0.01	1.63 ± 0.01	1.08 ± 0.01	0.51 ± 0.01
[0.3,0.45]	0.92 ± 0.01	1.32 ± 0.01	1.68 ± 0.01	1.78 ± 0.01	1.60 ± 0.01	1.06 ± 0.01	0.90 ± 0.03
[0.45,0.6]	1.19 ± 0.01	1.48 ± 0.01	1.77 ± 0.01	1.83 ± 0.01	1.62 ± 0.01	1.15 ± 0.01	...
[0.6,0.75]	1.30 ± 0.02	1.61 ± 0.01	1.87 ± 0.01	1.91 ± 0.01	1.63 ± 0.01	1.17 ± 0.01	...
[0.75,0.9]	...	1.72 ± 0.01	1.97 ± 0.01	1.96 ± 0.01	1.56 ± 0.01	1.80 ± 0.07	...
[0.9,1.05]	...	1.80 ± 0.01	2.07 ± 0.01	1.95 ± 0.01	1.53 ± 0.01	...	...
[1.05,1.2]	...	1.75 ± 0.01	2.04 ± 0.01	1.81 ± 0.01	1.42 ± 0.02	...	...
[1.2,1.35]	...	1.60 ± 0.02	1.78 ± 0.01	1.67 ± 0.01	...	...	...

First Observation of $\Lambda\pi^+$ and $\Lambda\pi^-$ Signals near the KN^- $(\mathrm{I}=1)$ Mass Threshold in the $\Lambda_c^+ \to \Lambda\pi^+\pi^+\pi^-$ decay

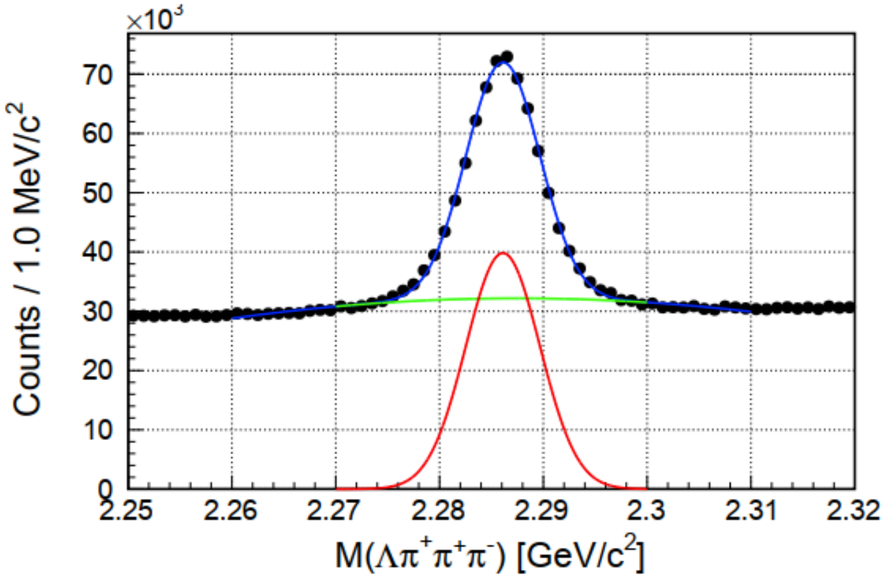

FIG. 2. The invariant mass of the $\Lambda\pi^+\pi^+\pi^-$ system after event selection. The green, red and blue curves represent the background, signal and total fit function, respectively. See text for details.

Flatt´e parametrization

$$
\begin{aligned}
& f_{Fl} \\
&= \frac{\Gamma}{(E - m_{\bar{K}N} - E_{\mathrm{BW}})^2 + (\Gamma + gk)^2/4}, E > m_{\bar{K}N} \\
&= \frac{\Gamma}{(E - m_{\bar{K}N} - E_{\mathrm{BW}} - g\kappa/2)^2 + \Gamma^2/4}, E < m_{\bar{K}N},
\end{aligned}
\tag{3}
$$

where E, E_{BW}, and Γ have the same definition as in Eq. (1), g is the coupling constant to $\bar{K}N$, and k (κ) is the magnitude of the $\bar{K}N$ relative momentum above (below) threshold as defined in Eq. (2). However, it is known that the three parameters (E_{BW}, Γ, and g) in Flatté parametrization are not independent, but are correlated by the so-called scaling behavior [11].

In particular, by neglecting the Λ_c^+ decay form factor, the $\mathrm{\bar{K}N}$ cusp can be related to the $\mathrm{\bar{K}-N}$ complex scattering length (A = a+ib) with the Dalitz model.

The Dalitz model

$$f_D = \frac{4\pi b}{(1+kb)^2+(ka)^2}, E > m_{\bar{K}N}$$
$$= \frac{4\pi b}{(1+\kappa a)^2+(\kappa b)^2}, E < m_{\bar{K}N},$$

where k and κ are the magnitude of the $\bar{K}N$ relative momentum above and below threshold, respectively. Specifically, $k = \sqrt{2\mu(E-m_{\bar{K}N})}$ for $E > m_{\bar{K}N}$ and $\kappa = \sqrt{2\mu(m_{\bar{K}N}-E)}$ for $E < m_{\bar{K}N}$, where $\mu = 1/(1/m_N + 1/m_{\bar{K}})$ is the reduced mass of the $\bar{K}N$ system.

First Observation of $\Lambda\pi^+$ and $\Lambda\pi^-$ Signals near the KN^- $(\mathrm{I} = 1)$ Mass Threshold in the $\Lambda_c^+ \to \Lambda\pi^+\pi^+\pi^-$ decay

TABLE III. Systematic uncertainties for the Breit-Wigner fitting parameters in [MeV].

Source	Mode	E_{BW} [MeV/c^2]	Γ [MeV/c^2]
Energy scale	$\Lambda\pi^+$	$+0.5$	-0.1
Resolution	$\Lambda\pi^+$	0.0	$+0.1$
Fitting procedure	$\Lambda\pi^+$	$+0.8$	-5.3
Total	$\Lambda\pi^+$	$^{+0.9}_{-0.0}$	$^{+0.1}_{-5.3}$
Final value		±0.9	±5.3
Energy scale	$\Lambda\pi^-$	$+0.2$	-2.9
Resolution	$\Lambda\pi^-$	0.0	$+0.1$
Fitting procedure	$\Lambda\pi^-$	-2.5	-23.4
Total	$\Lambda\pi^-$	$^{+0.2}_{-2.5}$	$^{+0.1}_{-23.6}$
Final value		±2.5	±23.6

TABLE IV. Systematic uncertainties for the Dalitz fitting parameters in [fm].

Source	Mode	a [fm]	b [fm]
Energy scale	$\Lambda\pi^+$	$+0.03$	-0.17
Resolution	$\Lambda\pi^+$	-0.01	-0.03
Fitting procedure	$\Lambda\pi^+$	$+0.37$	$+2.54$
Model	$\Lambda\pi^+$	$+0.05$	-0.05
Total	$\Lambda\pi^+$	$^{+0.38}_{-0.01}$	$^{+2.54}_{-0.18}$
Final value		±0.38	±2.54
Energy scale	$\Lambda\pi^-$	$+0.19$	-0.10
Resolution	$\Lambda\pi^-$	-0.01	0.00
Fitting procedure	$\Lambda\pi^-$	$+1.55$	-0.17
Model	$\Lambda\pi^-$	-0.16	-0.05
Total	$\Lambda\pi^-$	$^{+1.56}_{-0.16}$	$^{+0.00}_{-0.20}$
Final value		±1.56	±0.20

Combine the Belle & Belle II branching fractions.

$$r = \frac{r_1\sigma_2^2 + r_2\sigma_1^2}{\sigma_1^2 + \sigma_2^2 + (r_1 - r_2)^2\epsilon_r^2},$$

$$\sigma = \sqrt{\frac{\sigma_1^2\sigma_2^2 + (r_1^2\sigma_2^2 + r_2^2\sigma_1^2)\epsilon_r^2}{\sigma_1^2 + \sigma_2^2 + (r_1 - r_2)^2\epsilon_r^2}},$$

where r_i,σ_i, and ϵ_i are the branching fraction ratio, uncorrelated uncertainty, and relative correlated systematic uncertainty of the branching fraction ratio from each data sample, respectively.

Search for CP violation and measurement of branching fractions and decay asymmetry parameters for $\Lambda_c^+ \to \Lambda h^+$ and $\Lambda_c^+ \to \Sigma^0 h^+$ ($h = K, \pi$)

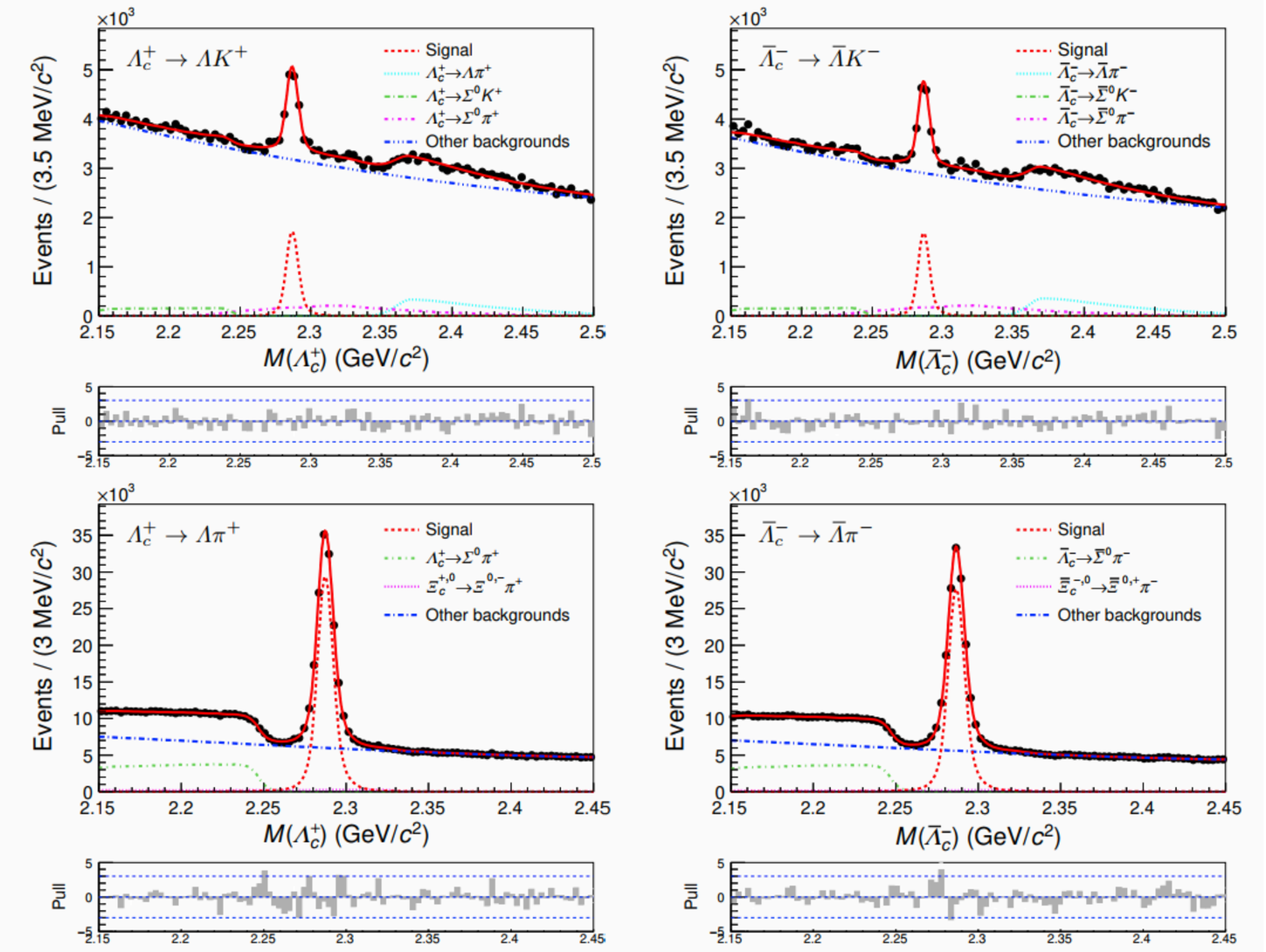

FIG. 1. The simultaneous fit to Λ_c^+ (left) and $\bar{\Lambda}_c^-$ (right) samples from real data for $\Lambda_c^+ \to \Lambda K^+$ (top) and $\Lambda_c^+ \to \Lambda \pi^+$ (bottom). The red curve is the total fitting result. The dashed lines show the components of signal and backgrounds (see text).

To measure the corrected raw asymmetries, we perform an unbinned extended maximum likelihood fit on the $M(\Lambda_c^\pm)$ distributions of the weighted Λ_c^+ and $\bar{\Lambda}_c^-$ samples simultaneously.

Search for CP violation and measurement of branching fractions and decay asymmetry parameters for $\Lambda_c^+ \to \Lambda h^+$ and $\Lambda_c^+ \to \Sigma^0 h^+$ ($h = K, \pi$)

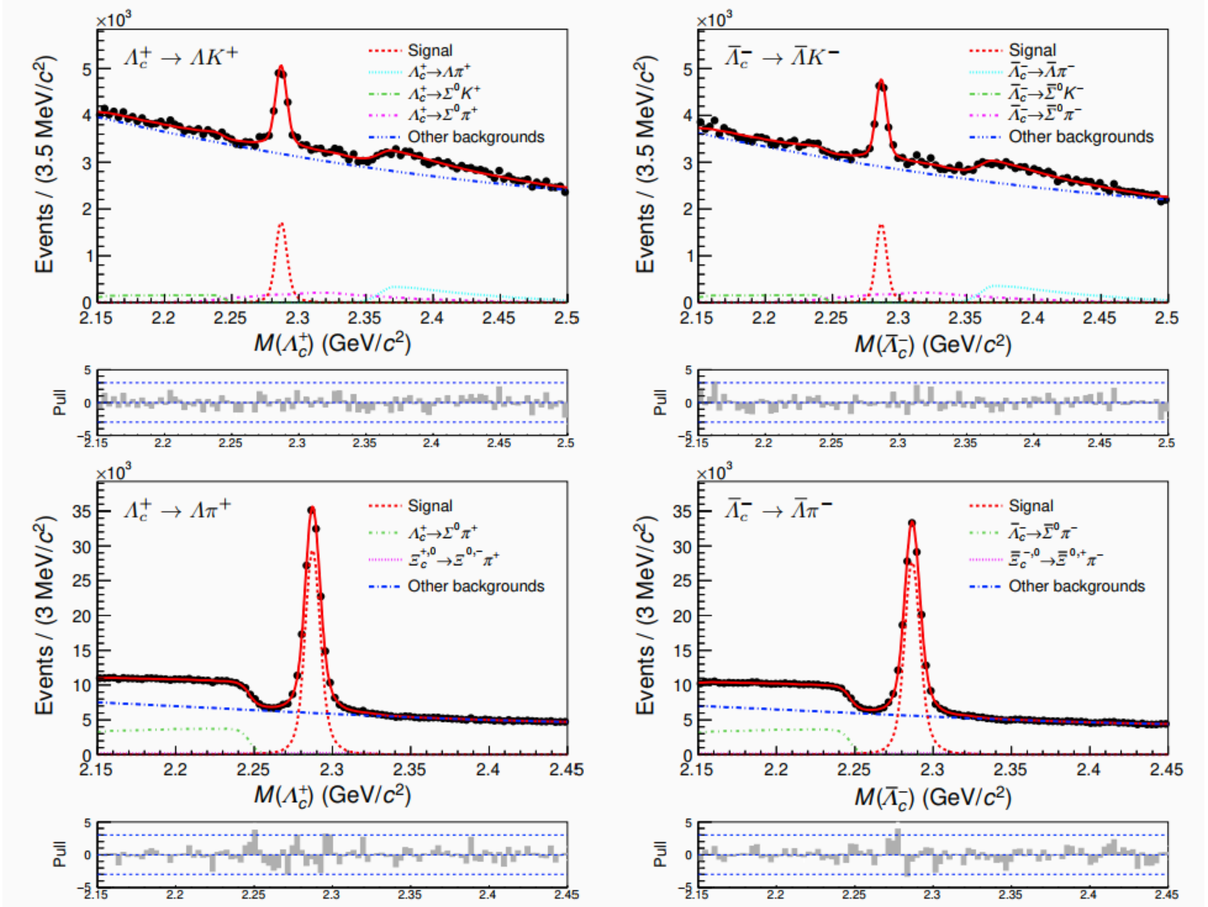

FIG. 1. The simultaneous fit to Λ_c^+ (left) and $\bar{\Lambda}_c^-$ (right) samples from real data for $\Lambda_c^+ \to \Lambda K^+$ (top) and $\Lambda_c^+ \to \Lambda \pi^+$ (bottom). The red curve is the total fitting result. The dashed lines show the components of signal and backgrounds (see text).

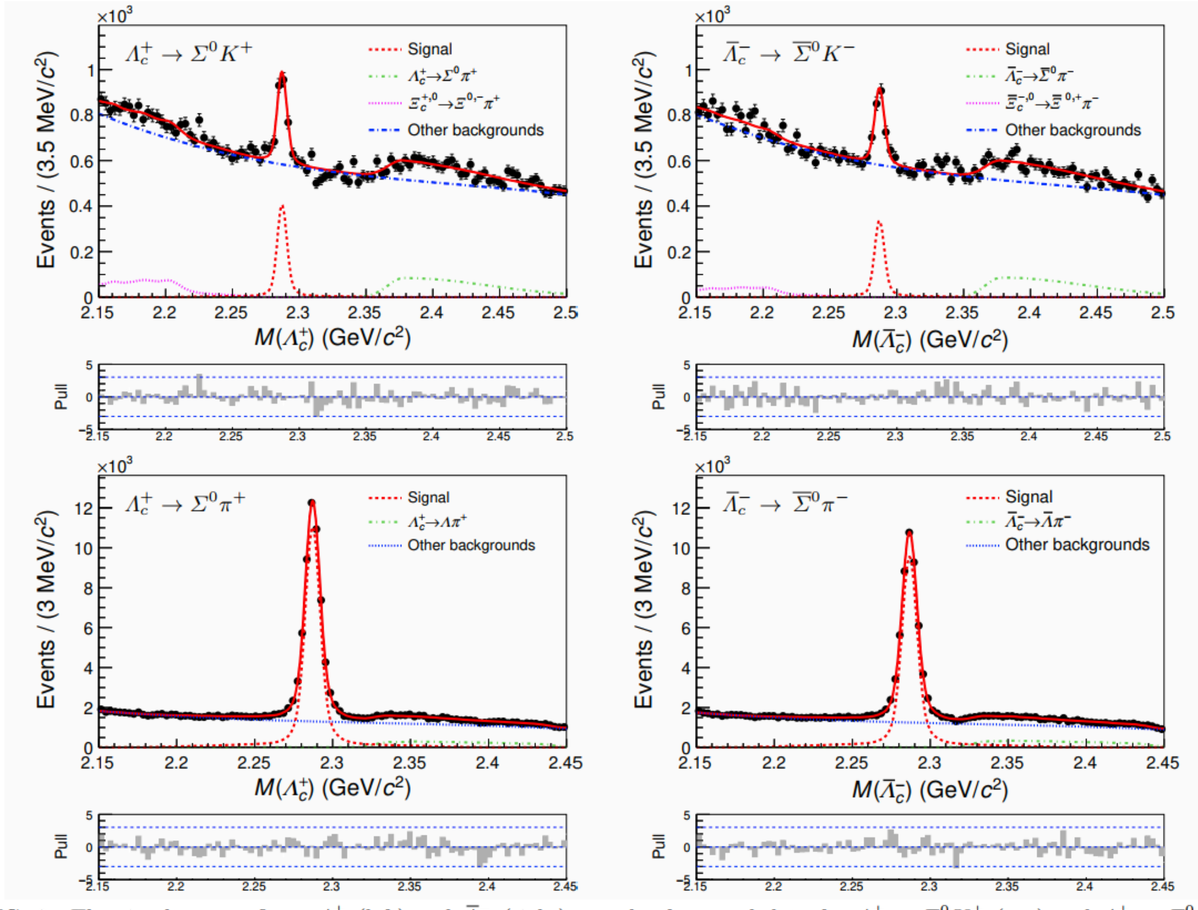

FIG. 2. The simultaneous fit to Λ_c^+ (left) and $\bar{\Lambda}_c^-$ (right) samples from real data for $\Lambda_c^+ \to \Sigma^0 K^+$ (top) and $\Lambda_c^+ \to \Sigma^0 \pi^+$ (bottom). The red curve is the total fitting result. The dashed lines show the components of signal and backgrounds (see text).

Search for CP violation and measurement of branching fractions and decay asymmetry parameters for $\Lambda_c^+ \to \Lambda h^+$ and $\Lambda_c^+ \to \Sigma^0 h^+$ ($h = K, \pi$)

TABLE III. The absolute systematic uncertainties (in units of 10^{-3}) for CP asymmetry $A_{CP}^{\rm dir}$.

Sources	$A_{CP}^{\rm dir}(\Lambda_c^+ \to \Lambda K^+)$	$A_{CP}^{\rm dir}(\Lambda_c^+ \to \Sigma^0 K^+)$
$A_\varepsilon^{K^+}$ map	$^{+0.8}_{-0.2}$	± 0.4
$A_\varepsilon^{\pi^+}$ map	± 0.4	$^{+0.5}_{-2.5}$
Signal shape	± 0.5	± 1.4
Background shape	-0.2	-3.1
Fit bias	$+0.6$	$+2.6$
Λ asymmetry	-0.2	-0.4
Total	$^{+1.2}_{-0.7}$	$^{+3.0}_{-4.3}$

TABLE IV. Relative systematic uncertainties (in units of %) for branching fractions.

Sources	$\frac{\mathcal{B}(\Lambda_c^+ \to \Lambda K^+)}{\mathcal{B}(\Lambda_c^+ \to \Lambda \pi^+)}$	$\frac{\mathcal{B}(\Lambda_c^+ \to \Sigma^0 K^+)}{\mathcal{B}(\Lambda_c^+ \to \Sigma^0 \pi^+)}$
PID efficiency correction	1.7	1.7
Signal shape	0.2	0.4
Background shape	–	0.1
BCS effect	0.1	0.4
Efficiency ratio	0.2	0.4
Total	1.7	1.8

Search for CP violation and measurement of branching fractions and decay asymmetry parameters for $\Lambda_c^+ \to \Lambda h^+$ and $\Lambda_c^+ \to \Sigma^0 h^+$ ($h = K, \pi$)

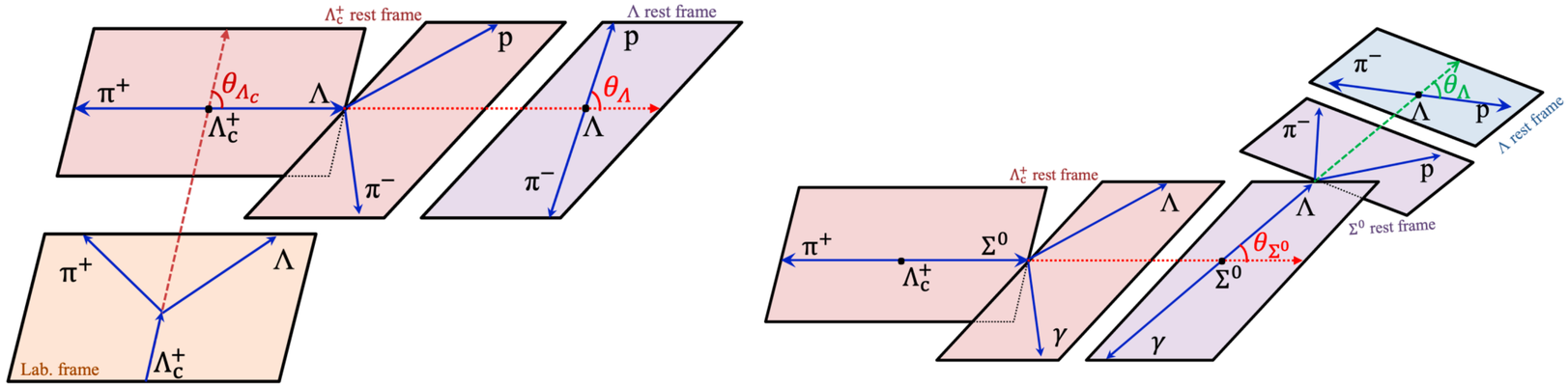

FIG. 5. Schematic plot showing the helicity angles: (left) $\theta_{\Lambda_c^+}$ and θ_Λ in $\Lambda_c^+ \to \Lambda\pi^+$, $\Lambda \to p\pi^-$; and (right) θ_{Σ^0} and θ_Λ in $\Lambda_c^+ \to \Sigma^0\pi^+$, $\Sigma^0 \to \gamma\Lambda$, $\Lambda \to p\pi^-$.

Search for CP violation and measurement of branching fractions and decay asymmetry parameters for $\Lambda_c^+ \to \Lambda h^+$ and $\Lambda_c^+ \to \Sigma^0 h^+$ ($h = K, \pi$)

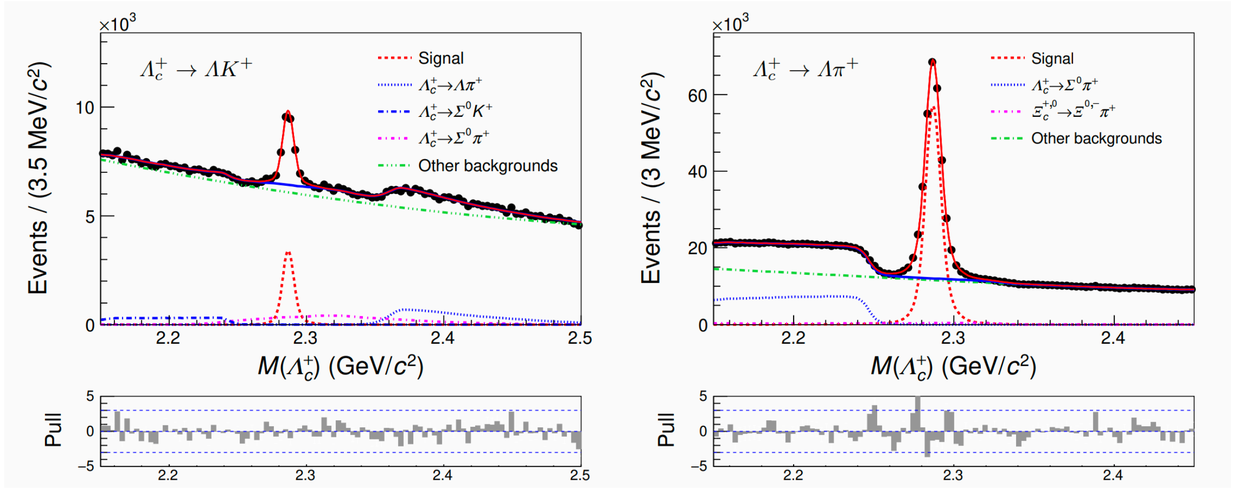

FIG. 6. The fit results of Λ_c^+ invariant mass distributions for $\Lambda_c^+ \to \Lambda K^+$ and $\Lambda_c^+ \to \Lambda \pi^+$ decays. The red curve shows the total fit result, and the blue curve the total background; the dashed curves show the components of signal and backgrounds. The fit qualities, χ^2 divided by the number of degrees of freedom, are $\chi^2/91 = 1.12$ and $\chi^2/91 = 1.38$, respectively.

Fit for real data.

$$\mathcal{B}(\Lambda_c^+ \to \Lambda K^+) = (6.57 \pm 0.17 \pm 0.11 \pm 0.35) \times 10^{-4},$$

$$\mathcal{B}(\Lambda_c^+ \to \Sigma^0 K^+) = (3.58 \pm 0.19 \pm 0.06 \pm 0.19) \times 10^{-4},$$

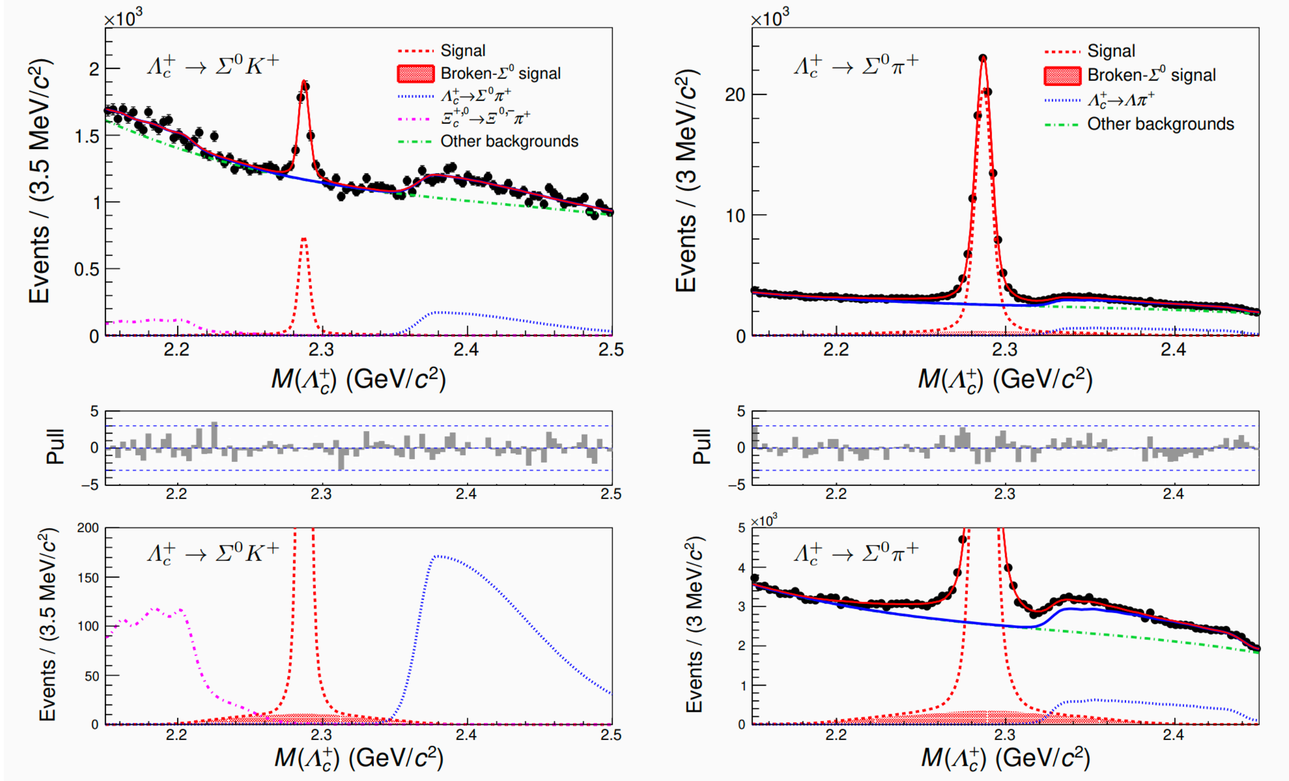

FIG. 7. The fit results of Λ_c^+ invariant mass distributions for $\Lambda_c^+ \to \Sigma^0 K^+$ and $\Lambda_c^+ \to \Sigma^0 \pi^+$ decays. The red curve shows the total fit result, and the blue curve the total background; the dashed curves show the components of signal (including the broken-Σ^0 signal) and backgrounds. The fit qualities, χ^2 divided by the number of degrees of freedom, are $\chi^2/91 = 1.38$, and $\chi^2/92 = 1.07$, respectively. The bottoms figures are the enlarged view to show the distributions of broken-Σ^0 signal (red-filled histogram) and the peaking backgrounds more clearly.

Search for CP violation and measurement of branching fractions and decay asymmetry parameters for $\Lambda_c^+ \to \Lambda h^+$ and $\Lambda_c^+ \to \Sigma^0 h^+$ ($h = K, \pi$)

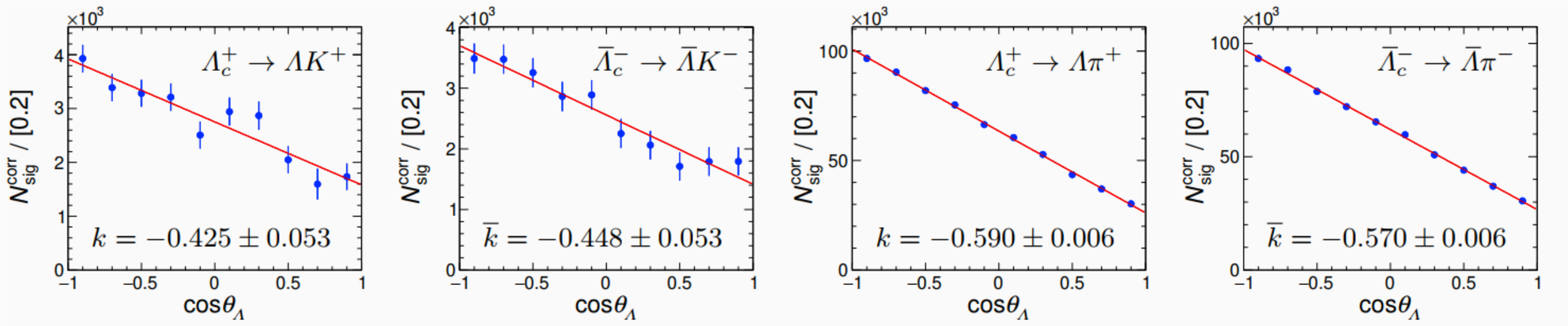

FIG. 8. The $\cos\theta_\Lambda$ distributions of $\Lambda_c^+ \to \Lambda K^+$ and $\Lambda_c^+ \to \Lambda \pi^+$ after efficiency-correction. We fit it with a linear function of $1 + \alpha_{\Lambda_c^\pm} \alpha_\mp \cos\theta_\Lambda$ with the χ^2 divided by the number of degrees of freedom, $\chi^2/9 = 1.04$, 0.57, 1.25, and 0.88, respectively, and the fitted slope values ($k = \alpha_{\Lambda_c^+} \alpha_-$ and $\bar{k} = \alpha_{\bar{\Lambda}_c^-} \alpha_+$) are shown.

Search for CP violation and measurement of branching fractions and decay asymmetry parameters for $\Lambda_c^+ \to \Lambda h^+$ and $\Lambda_c^+ \to \Sigma^0 h^+$ ($h = K, \pi$)

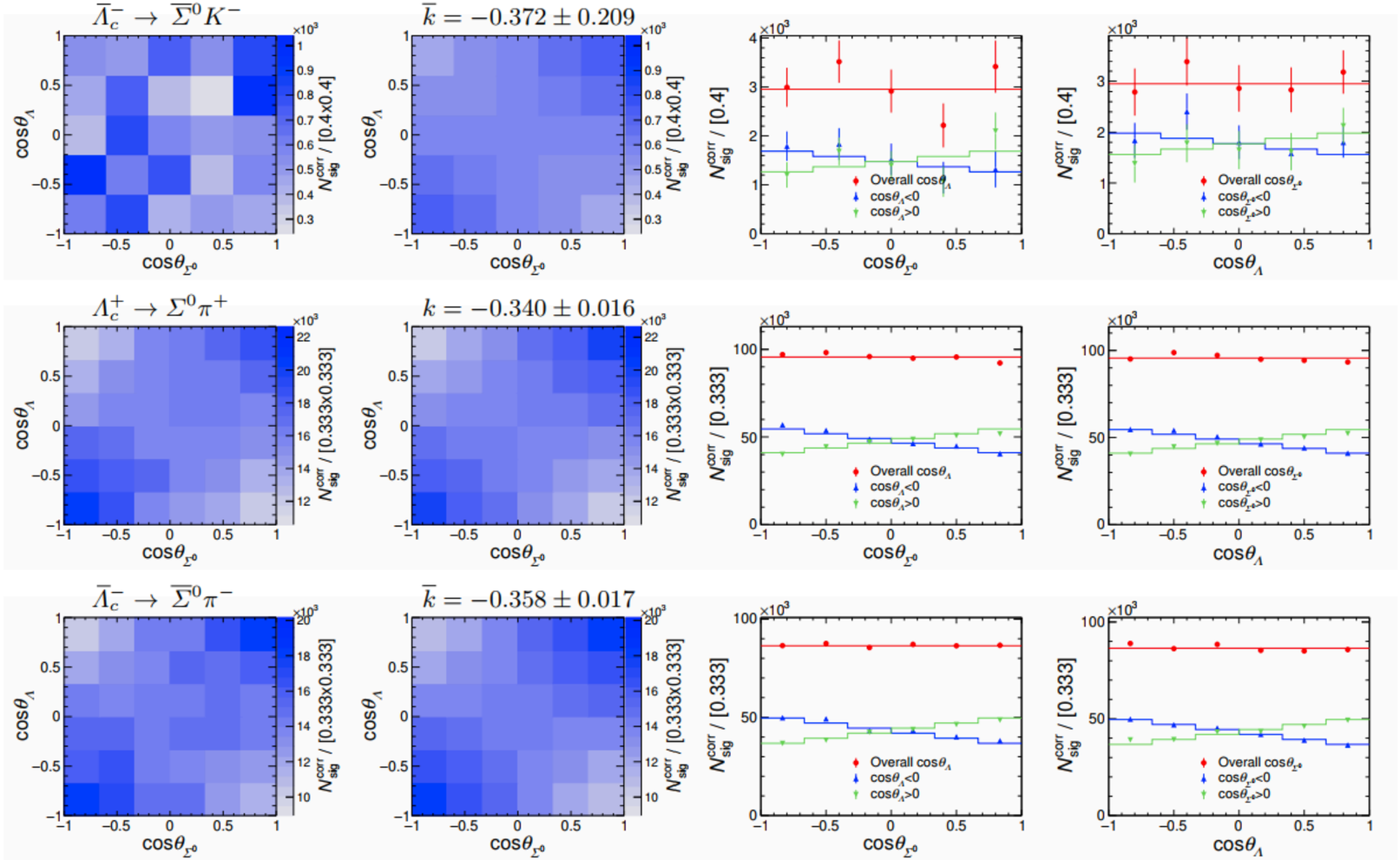

FIG. 9. The $[\cos\theta_{\Sigma^0}, \cos\theta_\Lambda]$ distributions of (upper plots) $\Lambda_c \to \Sigma K$ and (lower plots) $\Lambda_c \to \Sigma\pi$ decays. The first column shows the distributions after efficiency correction; the second column shows the respective fit results using a linear function $1 - \alpha_{\Lambda_c^\pm}\alpha_\mp \cos\theta_{\Sigma^0}\cos\theta_\Lambda$. Fitted slope values ($k = \alpha_{\Lambda_c^+}\alpha_-$ and $\bar{k} = \alpha_{\bar{\Lambda}_c^-}\alpha_+$) are shown. The χ^2 divided by the number of degrees of freedom is $\chi^2/24 = 0.82$ and 0.78 for the ΣK fits and $\chi^2/35 = 1.35$ and 1.05 for the $\Sigma\pi$ fits. The third column shows the projections of the $\cos\theta_{\Sigma^0}$ distributions (point with error) and the fit results (histograms) in overall (red) or negative (blue) or positive (green) $\cos\theta_\Lambda$ region; verse visa in forth column. The absolute slopes of all projections in slices equal half of the fitted slope listed in the second column.

Measurement of the Λ_c^+ lifetime

Table I: Systematic uncertainties on the Λ_c^+ lifetime.

Source	Uncertainty [fs]
Ξ_c contamination	0.34
Resolution model	0.46
Non-Ξ_c backgrounds	0.20
Detector alignment	0.46
Momentum scale	0.09
Total	0.77

Reconstruction of charged particles at Belle II relies on periodic calibrations to correct for detector misalignment and surface deformations of the internal components of the PXD and SVD, as well as for relative alignments of the tracking system [30]. Detector misalignment can bias measured particle decay lengths and therefore their decay times. To account for imperfections in the detector alignment, sets of signal-only simulated data, each with a size comparable to the collision data, are produced with detectors randomly misaligned according to the alignment precision observed in data. The root mean square dispersion of the lifetime residuals in these misaligned simulated data sets is 0.46 fs, which is taken as a systematic uncertainty due to imperfect detector alignment.